

Review

Insights into the roles of the Sideroflexins / SLC56 family in iron homeostasis and iron-sulfur biogenesis

Nesrine Tifoun^{1‡}, José M. De las Heras^{1‡}, Arnaud Guillaume¹, Sylvina Bouleau¹, Bernard Mignotte^{1,2} and Nathalie Le Floch^{1,3*}

¹ Université Paris-Saclay, UVSQ, LGBC, 78000, Versailles, France.

² École Pratique des Hautes Études, PSL University, 75014, Paris, France

³ IUT de Vélizy/campus de Rambouillet, GCGP Department, 19, allée des Vignes, 78120 Rambouillet, France

[‡] These authors equally contributed to this work.

* Correspondence: nathalie.leleu@uvsq.fr

Abstract: Sideroflexins (SLC56 family) are highly conserved multi-spanning transmembrane proteins inserted in the inner mitochondrial membrane in eukaryotes. Few data are available on their molecular function but, since their first description, they were thought to be metabolite transporters probably required for iron utilization inside the mitochondrion. Such as numerous mitochondrial transporters, sideroflexins remain poorly characterized. The prototypic member SFXN1 has been recently identified as the previously unknown mitochondrial transporter of serine. Nevertheless, pending questions on the molecular function of sideroflexins remain unsolved, especially their link with iron metabolism. Here, we review the current knowledge on sideroflexins, their presumed mitochondrial functions and the sparse - but growing - evidence linking sideroflexins to iron homeostasis and iron-sulfur cluster biogenesis. Since an imbalance in iron homeostasis can be detrimental at the cellular and organismal levels, we also investigate the relationship between sideroflexins, iron and physiological disorders. Investigating Sideroflexins' functions constitutes an emerging research field of great interest and will certainly lead to main discoveries on mitochondrial physiopathology.

Keywords: sideroflexin; mitochondria; mitochondrial transporters; iron homeostasis; iron-sulfur cluster; heme biosynthesis; one-carbon metabolism; ferroptosis; ferritinophagy.

1. Sideroflexins: from structure to function

1.1. Sideroflexins from an historical point of view

The mitochondrion is at the crossroad of key metabolic pathways (energy metabolism, central carbon metabolism, one carbon metabolism, lipid, nucleotides and amino acids synthesis, etc.) and is a key player in cell fate and response to stress or infection. In order to ensure its essential functions within the cell, the mitochondrion requires a wide variety of enzymes and transporters. Among these proteins, sideroflexins (SFXN) form a family of recently discovered mitochondrial proteins whose cell functions are progressively being specified. The first mention of the name "sideroflexin" appeared in 2001 [1]. Since then, a few studies have been dedicated to SFXN proteins and, at the time we are writing this review, only 24 articles are retrieved in Pubmed using the keyword "sideroflexin". Pioneers in the SFXN field, Fleming *et al.* identified a mutation affecting the *Sfxn1* gene in the *flexed-tail* mouse and emitted the hypothesis that the loss of *Sfxn1* was responsible for the sideroblastic anemia phenotype. However, it should be noticed that the causal link between the mutation in the *Sfxn1* gene and the phenotype of *flexed-tail* mice has not been clearly established yet. It was even questioned following a study showing that *flexed-tail* mice also had a mutation of the *Madh5/Smad5* gene, involved in the BMP pathway, which could explain the anemia and *flexed-tail* phenotype [2,3].

Anyway, SFXN own their name to the mice in which they were discovered (SIDEROblastic anemia and FLEXed-tail mouse) [1].

1.2. The Sideroflexin family: from genes to proteins

Sideroflexins (forming the SFXN/SLC56 family of mitochondrial transporters [4]) are highly conserved throughout eukaryotes. Only one sideroflexin is found in yeast (Fsf1 for Fungal sideroflexin 1), whereas there are two SFXNs in *Drosophila* (dSfxn1/3 and dSfxn2) and five SFXN (SFXN1-5) in vertebrates [1,5–7]. Our purpose is not to give an extensive overview of SFXN tissue distribution in this review, but some data are available in the literature. For example, SFXN1 mRNA levels in normal tissues and human cancers, as well as tissue distribution of the five human SFXN, are available in [8].

SFXNs homologues display a high amino acid identity rate in mouse [1], xenopus [5] and human [8]. In humans, SFXN1 and SFXN3 share 76.56% identical amino acids whereas there is 56.05% identity between SFXN1 and SFXN2 and only 22.04% between SFXN1 and SFXN4. An alignment of human SFXNs is shown in **Figure 1**. Identity rates between the different human, *Drosophila* and yeast sideroflexins proteins are described elsewhere [8,9]. The high degree of homology between SFXNs, especially between SFXN1 and SFXN3 in humans, suggest that sideroflexins may ensure redundant functions, as it was proposed for the mitochondrial import of serine that seems to be mediated by SFXN1 [8]. This function will be evoked in more details below (see the section dedicated to the role of SFXN in regulating mitochondrial metabolism). Among the five mammalian SFXNs, SFXN4 is the most divergent member suggesting that this member do not share the same functions (**Figure 1**). Indeed SFXN4 was not able to suppress defects caused by the concomitant loss of SFXN1 and SFXN3 in mammalian cells [8]. Interestingly, up to date no study has been done to specifically uncover Fsf1 function. Because of the high degree of similarity between fungal sideroflexin and SFXN proteins from higher eukaryotes, we think that studies on the functions of Fsf1 will certainly lead to huge advances in the SFXN field and maybe reveal a general function for this family of proteins.

1.3. Sideroflexins are mitochondrial transporters implicated in one-carbon metabolism

SFXNs possess four to six predicted transmembrane domains composed by α -helices revealed by *in silico* modeling [1,6,7]. These proteins share several highly conserved motifs including a HPDT motif and an asparagine-rich sequence (**Figure 1**) [1,6]. The functions of those conserved motifs have not been uncovered yet. Recently, Gyimesi and Hediger performed an *in silico* analysis of human SFXN1-5 sequences and described six well-conserved regions that could be important for SFXNs activity [10]. Whether these conserved regions are essential for metabolite transport need to be further confirmed at the bench. To date, no crystal structure has been released for SFXNs. We thus tried to model SFXN tridimensional structure using the trRosetta software [11]. SFXN1 predicted structure is shown in **Figure 2**. Interestingly, this structure reveals six internal alpha helices that may correspond to the transmembrane domain of SFXN1.

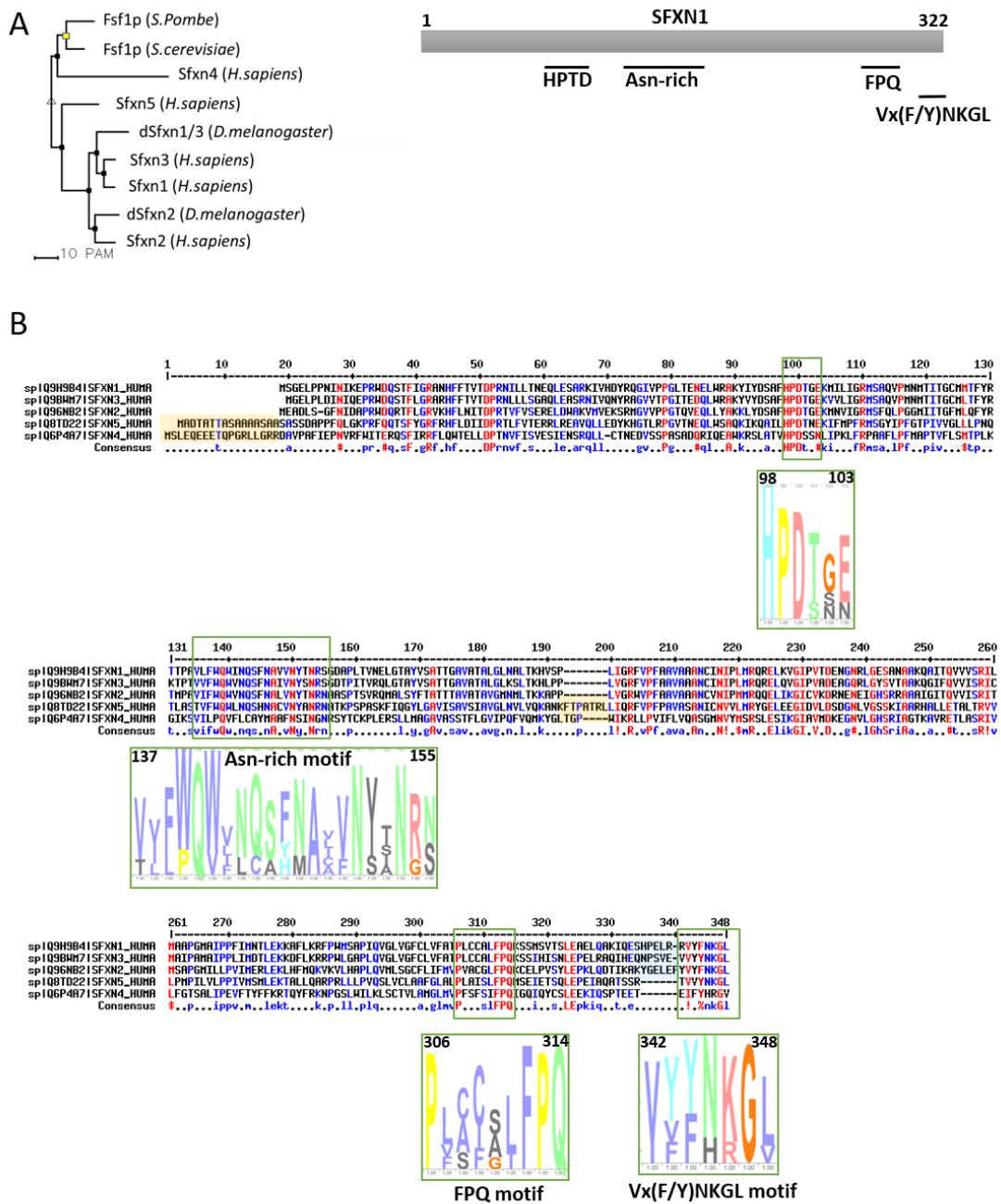


Figure 1. SFXNs form a family of conserved proteins in *Eukarya*. **A.** Left panel: Phylogenetic tree obtained using the MultiAlin software (<http://multalin.toulouse.inra.fr/multalin/>)[12]. Right panel: scheme of the SFXN1 protein and its conserved motifs. **B.** Alignment of human SFXNs protein sequences. Red amino acids are for high consensus levels (90%), the blue ones are for low consensus levels (50%). Meaning of symbols found in the consensus line: “!” is for Ile or Val, “\$” is for Leu or Met, “%” is for Phe or Tyr, “#” is anyone of Asn, Asp, Glu, Gln. Conserved motifs are shown and

highlighted using an HMM logo created using Skyline (<http://skylign.org/>) with consensus colors for amino acids according to the ClustalX coloring scheme.

SFXN1 topology was recently investigated by APEX and classical biochemical experiments [13–15]. Acoba *et al.* [15] performed detergent extraction and protease-protection assays on HEK human cells and confirmed that endogenous SFXN1 is a mitochondrial protein inserted in the inner mitochondrial membrane (IMM). Furthermore, evidence was given for the presence of N-terminus in the intermembrane space (IMS) but not in the matrix contrarily to what is predicted by a *in silico* analysis using Protter. According to biochemical data, the C-terminus seems to protrude in the matrix, in agreement with the previously proposed 5 transmembrane domains. However, our model is rather in agreement with a TM domain composed of six alpha helices and, if this predicted structure is correct, N and C termini could be in the same mitochondrial compartment (**Figure 2**). CryoEM structure of SFXN1 is thus needed to precise the three-dimensional structure of this carrier. Moreover, two recent studies investigated the mechanisms of SFXN1 mitochondrial import and shed light on the role of TIM22 and AGK2 in this process [16,15]. Evidence for a mitochondrial localization of SFXN1 are listed in the **Table 1**.

Because of their predicted structure, showing several hydrophobic alpha helices, and their mitochondrial location, sideroflexins were proposed to be mitochondrial metabolite transporters. Rat Sfxn3 was presumed to be a tricarboxylate carrier (TCC) and, later, Sfxn5 (also known as BBG-TCC) was reported to transport citrate *in vitro* [17,18]. However, it is only recently that a function of mitochondrial serine transporter was reported for SFXN1 [8].

By a bioinformatic analysis, the *S. cerevisiae* Fsf1 (YOR271cp) was proposed to be a candidate alpha-isopropylmalate transporter but no experimental data ascertained this function [19]. Similarly, the predicted Fsf1 protein from *Schizosaccharomyces pombe*, Spac17g6.15c, is annotated as a serine transporter in the database Pombase (<https://www.pombase.org/>) based on its homology with human SFXN1 [20,21], although it has not been extensively studied.

Since mice lacking Sfxn1 present similar features to that observed in human syndromes caused by a lack of pyridoxine or ALAS2 mutation (X-linked sideroblastic anemia), it was also proposed that Sfxn1 transports pyridoxine (B6 vitamin) inside the mitochondria [1,22]. Since pyridoxine is the precursor of pyridoxal phosphate that serves as a cofactor for ALAS2 (the erythroid specific enzyme catalyzing the first step of heme biosynthesis), SFXN1 could thus directly regulate heme biosynthesis. However, it has been recently reported that human SFXN1 is not able to transport pyridoxine *in vitro* [8]. Even if we cannot exclude that SFXN1 functions in a complex that is not fully reconstituted in *in vitro* assays, SFXN1 may not be the carrier for pyridoxine. Mtm1p, SLC25A39 yeast homologue, was suggested to import pyridoxal 5'-phosphate inside the mitochondria [23,24]. However, the substrate specificity of the SLC25A39 carrier remains unknown [25].

Thus, the main role of Sfxn1 seems to be the mitochondrial serine import. Inside the mitochondrion, Serine can be catabolized by the serine hydroxymethyl transferase (SHMT2) into glycine, an amino acid necessary for ALA synthesis (see below). So, the lack of Sfxn1 would lead to decreased mitochondrial levels of serine and glycine leading to ALA synthesis impairment (see section 4).

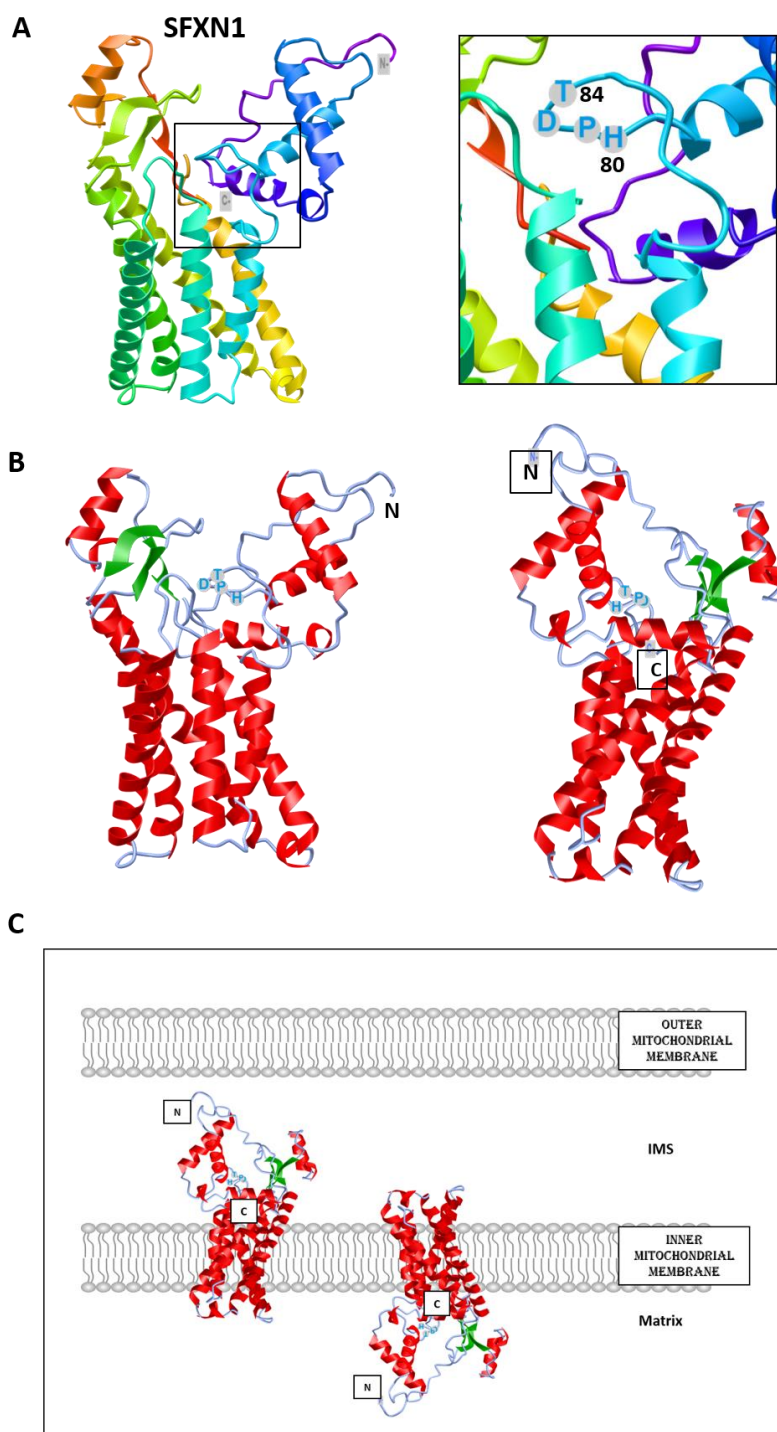


Figure 2. Predicted structure of human SFXN1. Structure prediction was obtained using trRosetta. The confidence of the predicted model shown here is very high (with estimated TM-score=0.806). The model was built by trRosetta based on *de novo* folding, guided by deep learning restraints. iCn3D was used for the visualization of 3D structure [26]. *A.* SFXN1 predicted structure reveals several alpha helices and beta strands. N and C termini are labelled. The inset shows the position of the HPDT motif (aa 80-83), located just after the fourth helix. *B.* Two views highlighting secondary structures (helices in red, beta sheets in green). *C.* Models for SFXN1 insertion in the inner mitochondrial membrane.

1

Table 1. Evidence for a mitochondrial localization of Sideroflexins

SFXN	Model	Localization	Experiment	Reference
SFXN1	Mouse	IMM	Co-fractionation	Fleming <i>et al.</i> , 2001 [1]
	Human cells (Jurkat, K562)		Immunoblot on affinity-purified mitochondria STED (co-localization of Flag-SFXN1 and COX4)	Kory <i>et al.</i> , 2018 [8]
	Human cells (MCF7, HT1080), <i>Drosophila</i>		Immunoblot on mitochondrial extracts (fractionation) Confocal microscopy, Proteomics (LC-MS/MS on SFXN1 IP)	Our unpublished data
	Human cells (HEK)		SILAC-based proteomics coupled LC-MS/MS, carbonate extraction, digitonin fractionation	Acoba <i>et al.</i> , 2020 [15]
SFXN2	Human cells (HeLa)	OMM	Confocal microscopy (Tom20 co-localization)	Mon <i>et al.</i> , 2018 [9]
	Human cells (Jurkat, K562)		Immunoblot on affinity-purified mitochondria	Kory <i>et al.</i> , 2018 [8]
	Human cells (HEK)		SILAC-based proteomics coupled LC-MS/MS	Acoba <i>et al.</i> , 2020 [15]
SFXN3	Rat embryonic brain cells	IMM	Fractionation, Confocal microscopy (co-localization with COX4), TEM	Rivell <i>et al.</i> , 2019 [27]
	Human cells (Jurkat, K562)		Immunoblot on affinity-purified mitochondria	Kory <i>et al.</i> , 2018 [8]
	Human cells (HEK)		SILAC-based proteomics coupled LC-MS/MS	Acoba <i>et al.</i> , 2020 [15]
	Human cells (HeLa)	IMM	Fractionation and protease protection assay	Hildick-Smith <i>et al.</i> , 2013 [28]
SFXN4	Human cells (Jurkat, K562)		Immunoblot on affinity-purified mitochondria	Kory <i>et al.</i> , 2018 [8]
	Human cells (HEK)		SILAC-based proteomics coupled LC-MS/MS	Acoba <i>et al.</i> , 2020 [15]
	Human cells (HEK)		SILAC-based proteomics coupled LC-MS/MS	Acoba <i>et al.</i> , 2020 [15]
SFXN5	Human cells (HEK)		SILAC-based proteomics coupled LC-MS/MS	Acoba <i>et al.</i> , 2020 [15]
	Mouse astrocytes, human cortex and spinal cord		Immunocapture of GFP-OMM-tagged mitochondria (MitoTag mice), immunostaining	Fecher <i>et al.</i> , 2019 [29]

2

¹IMM: inner mitochondrial membrane, IP: immunoprecipitation, OMM: outer mitochondrial membrane, STED: stimulated emission depletion, TEM: Transmission Electron

3

Microscopy, SILAC: Stable isotope labelling of amino acids, LC-MS/MS: Liquid chromatography and tandem mass spectrometry

4 1.4 Sideroflexins in disease

5 Hildick-Smith *et al.* described for the first time a human syndrome (combined oxidative
6 phosphorylation deficiency-18, OMIM entry # 615578), that was directly associated with the lack of a
7 member of the Sfxn family, namely SFXN4 [28]. Patients showed macrocytic anemia and
8 mitochondriopathy non-explainable by other causes but the lack of SFXN4. Recently, a third patient
9 with SFXN4 mutations was described by Sofou *et al* [30]. The three patients with SFXN4 mutations
10 presented with intrauterine growth retardation, mild to severe intellectual disabilities, microcephaly,,
11 neonatal lactic acidosis, macrocytic anemia and severe visual impairment. Sofou *et al* reported optic
12 nerve hypoplasia in the third case. More recently, some of the mechanisms that could explain those
13 effects in humans were reported in the K562 erythroleukemic cell line [31]. Interestingly SFXN4 loss-
14 of-function leads to a general decrease in the levels of the respiratory chain complexes I-IV, which
15 could be explained by an impaired Fe-S cluster synthesis, as evidenced by a Fe-S fluorescence assay
16 (FeSFA). Nevertheless, Sofou *et al.* showed that the effect of SFXN4 decrease would be exclusively in
17 Complex I but not in the rest of the respiratory chain complexes after muscle biopsy [30]. Despite
18 these discrepancies, which could be due to the different nature of the mutations analyzed in each
19 case, it seems clear that Complex I activity is affected in both studies, which reinforces the hypothesis
20 that SFXN4 could have a role, either direct or indirect, on Fe-S biosynthesis.

21 Besides the description of mutations in the *SFXN4* human gene causing the COXPD18 syndrome,
22 *SFXN4* was also reported to be a predisposition gene for familial colorectal cancer (CRC). Hence, rare
23 *SFXN4* truncating variants were identified in 3/96 CRC familial cases [32]. An aberrant expression of
24 *SFXN1* and *SFXN5* was also reported in patients with breast cancer or gliomas [33,34].

25 2. Sideroflexins and mitochondrial respiration

26 2.1. Overview of the mitochondrial respiratory complexes and the place of iron in RC

27 Oxidative Phosphorylation (OXPHOS) couples the transport of electrons (through a series of
28 mitochondrial respiratory complexes containing redox-active prosthetic groups) to the production of
29 ATP by the mitochondrial ATP synthase, commonly referred to as the complex V of respiratory chain
30 (**Figure 3**). Respiratory complexes (RC) are arranged in supercomplexes (SC) and megacomplexes in
31 the inner mitochondrial membrane [35,36]. The Electron Transport Chain (ETC) comprises four RC
32 (Complex I-IV) containing more than 70 nuclear DNA encoded subunits and 13 mitochondrial DNA
33 (mtDNA) encoded subunits, some of which including iron-sulfur clusters (ISCs) or heme; those iron-
34 containing groups are essential cofactors for electron transport from one complex to another [37,38].
35 The purpose of this review is not to give an extensive overview of the abundant literature on RC, so
36 we invite the reader to refer to recent reviews for details on the composition, structure and biogenesis
37 of RC [35,38,39].

38 Mammalian Complex I (NADH: Ubiquinone Oxidoreductase) is a L-shaped megastructure of
39 about 1 MDa comprising 14 core subunits and up to 45 subunits. Among them, five essential subunits
40 (NDUFV1, NUDFV2, NDUFS1, NDUFS7 and NDUFS8) bare the eight ISCs of CI (two [2Fe-2S] and
41 six [4Fe-4S] clusters).

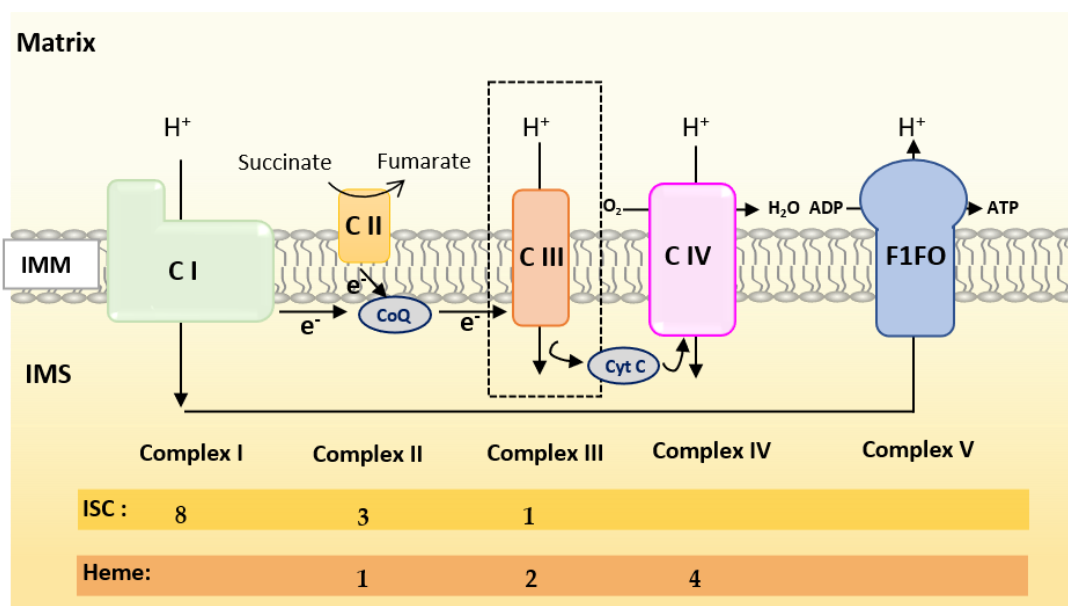
42 Mammalian Complex II, the smallest of the RC, is composed of only four subunits: succinate
43 dehydrogenase [ubiquinone] flavoprotein (also known as Flavoprotein subunit of complex II, Fp,
44 SDHA), succinate dehydrogenase [ubiquinone] iron-sulfur subunit (a Fe-S protein also named Ip or
45 SDHB), the membrane-anchoring succinate dehydrogenase cytochrome b560 subunit (CybL, SDHC),
46 and finally the succinate dehydrogenase [ubiquinone] cytochrome b small subunit (CybS, SDHD).
47 These subunits are respectively encoded by the *SDHA*, *SDHB*, *SDHC* and *SDHD* nuclear genes.
48 Fp/SDHA and Ip/SDHB are anchored to the IMM thanks to CybL/SDHC and CybS/SDHD that are
49 the membrane-anchoring subunits of CII. Complex II contains three ISCs ([2Fe-2S], [4Fe-4S] and [3Fe-
50 4S] in SDHB) and a heme shared by SDHC and SDHD.

51 Mammalian Complex III (also known as bc1 complex) is a dimer made of monomers containing
52 11 subunits among which three are essential redox subunits: cytochrome b, cytochrome c1 and the
53 Fe-S protein Cytochrome b-c1 complex subunit Rieske (Rieske, ISP, RISP, Rip1 are alternative names

54 that can be found in the literature for this protein). Altogether, these catalytic subunits possess two
 55 heme b (Cyt b), a c-type heme (Cyt c1) and a [2Fe-2S] cluster (Rieske) [40]. Heme b is synthesized by
 56 Ferrochelatase (FECH) but the mechanism of its insertion into cytochrome b has not been fully
 57 elucidated [40].

58 Mammalian Complex IV contains three mitochondrially-encoded subunits (Cytochrome c
 59 oxidase subunit 1, 2 and 3) plus eleven subunits encoded by the nuclear genome. CIV possesses four
 60 redox-active metal centers including heme a and heme a3 but no ISCs.

61 To summarize, Complex I is made of numerous subunits including 8 ISC-containing subunits
 62 but none containing heme. Complex IV presents 4 redox-active centers containing heme but no ISC.
 63 Both Complexes II and III have ISC and heme containing subunits.



64 **Figure 3.** Scheme of the mitochondrial respiratory chain. ISC and heme indicate the respective number
 65 of ISC-containing subunits and heme in each complex.

66 2.2. Current knowledge on the regulation of mitochondrial respiration by SFXN proteins

67 Kory *et al.* reported decreased basal respiration in SFXN1/SFXN3 double knockout Jurkat cells
 68 [8]. Whereas SFXN1 loss alone is not detrimental for respiration of intact cells [8,15], Acoba *et al.*
 69 reported a significant decrease in Oxygen Consumption Rates (OCR) of isolated mitochondria from
 70 HEK SFXN1 KO cells with CI, CII and CIII substrates (pyruvate, Glu, Gln, dimethyl- α -ketoglutarate,
 71 succinate and glycerol-3-phosphate) [15]. In human embryonic cells, the loss of SFXN1 leads to a
 72 marked decrease in the protein levels of three subunits of the Complex III and to a lesser extent in
 73 Complex II subunit SDHB (**Table 2**) [15]. SFXN4 KO leukemic cells also showed reduced levels of
 74 several RC subunits containing ISCs [31].

75 Whereas no significant change in the activity of the CI, CII and CIV ETC complexes was
 76 observed upon SFXN1 gene knockout in HEK cells, CIII activity was dramatically decreased and
 77 partially restored upon SFXN1 overexpression [15]. In agreement with the observed decrease in the
 78 levels of cytochrome b (MT-CYB), cytochrome b-c1 complex subunit 2 (UQCRC2) and cytochrome b-
 79 c1 complex subunit Rieske (UQCRC1) subunits, Acoba *et al.* also reported a reduction in CIII2 and
 80 in CIII2-CIV subcomplex whereas the assembly of respiratory supercomplexes was unaffected.
 81 Mitochondrial translation is not dramatically impaired in the absence of a functional SFXN1 protein,
 82 nevertheless a slight decrease in cytochrome b translation was reported in this study.

83 No decrease neither in the quantity of mtDNA nor in the mitochondrial mass was seen in SFXN1
 84 KO cells, thus a general defect in mitochondrial biogenesis can be excluded [8,15]. Current knowledge
 85 on Complex III biogenesis is well-described in [40]. Seven assembly factors are implicated in CIII
 86 biogenesis in humans (UQCC1-3, CCHL, BCSL1, LYRM7 and TTC19). The Rieske subunit is first

87 translocated from the cytosol to the matrix where it acquires its ISC and is further incorporated in
88 CIII. In the matrix, Rieske is stabilized by the chaperone LYRM7 [41]. BCS1L is required for the
89 translocation of the folded Rieske iron-sulfur protein in the IMM by a mechanism that remains largely
90 unknown [42]. No regulation of the levels of BCSL1 and LYRM7 assembly factors was observed when
91 SFXN1 is absent in mammalian cells [15].

92 Interestingly, HEK *SFXN1*^{KO} cells were reported to have markedly reduced levels of Coenzyme
93 Q (CoQ, ubiquinone), a lipid of the IMM which accepts electron from CI and CII and then donates
94 one electron to the ISC of the Rieske subunit and another one to the heme of the cytochrome b of CIII
95 (see [40] and [43] for more details on the transfer of electrons from CoQ to the IMS soluble electron
96 carrier cytochrome c).

97 Deficiencies of mitochondrial respiration and/or RC activity were also reported for other SFXN, as
98 summarized in **Table 2**. For example, *SFXN2* knockout led to a decreased activity of CII-CIII and CIV
99 [9]. As no specific impairment in complex III activity has been described nor in *SFXN2* nor in *SFXN4*
100 KO cells, there is presumably no interaction between those SFXN isoforms and the BCS1L protein
101 (responsible of the GRACILE Syndrome), a mitochondrial chaperone which is anchored to the inner
102 mitochondrial membrane and required for proper Complex III activity [44]. Nevertheless, this
103 possibility cannot be totally discarded, as the patients with S78G point mutation in the BCS1L gene
104 have no decreased Complex III activity when compared with other mutations of the same gene.

105

106 **Table 2.** Consequences of SFXN deficiency on the ETC complexes

SFXN	Model	Complex	Data	Reference
SFXN1	HEK <i>SFXN1</i> ^{KO} cells HeLa <i>SFXN1</i> ^{KO} cells	CI	No significant loss of activity	Acoba <i>et al</i> , 2020 [15]
		CII	No significant loss of activity SDHB ↓ UQCRC2 ↓↓ UQCRC1 ↓↓	
		CIII	Cytochrome b ↓↓↓ Significant loss of activity Reduced levels of CIII ₂ and CIII ₂ -CIV respiratory complexes	
SFXN2	HEK <i>SFXN2</i> ^{KO} cells	CI CII- CIII CIV	No significant loss of activity Significant loss of activity Significant loss of activity	Mon <i>et al</i> , 2019 [9]
SFXN3	<i>SFXN3</i> KO mouse	CI, CIV	No significant loss of activity	Amorim <i>et al</i> , 2017 [45]
SFXN4	Primary fibroblasts from two individuals with <i>SFXN4</i> mutations <i>SFXN4</i> KD zebrafish K562 <i>SFXN4</i> ^{KO} cells	CI+CIII	Decreased activity	Hildick-Smith <i>et al</i> , 2013 [28]
		CI CI+CIII	Decreased activity	
		CI CII CIII CIV	NDUFB8 ↓ SDHB ↓ UQCRC2 ↓ COX2 ↓	
SFXN5			N.A. ¹	Paul <i>et al</i> , 2019 [31]

¹ NA: Not addressed

108 3. Which place for Sideroflexins in the regulation of mitochondrial metabolism?

109 3.1 Sideroflexins and one-carbon metabolism (OCM)

110 Using CRISPR/Cas9 based-screening, Kory *et al.* uncovered a function of mitochondrial serine
111 transporter for SFXN1 [8]. The import of serine inside mitochondria is a key step of the OCM, a major
112 metabolic pathway coupled to the synthesis of methyl donors necessary for purine synthesis,
113 epigenetic methylation processes and synthesis of neurotransmitters [46]. Moreover, glycine - arising
114 from serine catabolism by the SHMT2 enzyme [47] - is a key amino acid for the synthesis of heme, a
115 cofactor present in cytochromes of the respiratory chain and other essential proteins, such as CYP450
116 proteins. Finally, OCM is known as a central pathway ensuring hyperproliferation of cancer cells.
117 Hence OCM, through the folate cycle, links serine catabolism to purine and nucleotides biosynthesis.
118 Liver, kidney and blood are tissues with high OCM activity, however OCM role is not restricted to
119 these organs but present in all human tissues including brain [46]. Actually, defective one-carbon
120 metabolism during embryonic development is responsible for neural tube defects.

121 Whereas Jurkat cells lacking SFXN1 proliferate as wild-type cells do, their proliferation rate is
122 markedly reduced in a medium lacking serine but is normal in the absence of glycine that can be
123 provided by the catabolism of serine [8]. A lower proliferative rate compared to that of wild-type
124 cells was also reported for HEK *SFXN1* KO cells in the absence of serine. Interestingly, proliferation
125 of SFXN1 deficient cells was enhanced when formate (OCM metabolite), but not hemin (heme
126 derivative), was added [15]. Additionally, Kory *et al.* showed that the double knockout of SFXN1 and
127 SFXN3 greatly impaired proliferation in a glycine-deficient medium. Apart from human *SFXN4*,
128 overexpression of virtually any *SFXN* family member including *S. cerevisiae* FSF1/YOR271C and the
129 two *Drosophila* orthologues *dSfxn1* and *dSfxn2* can rescue the glycine auxotrophy due to the OCM
130 defect induced by the concomitant loss of SFXN1 and SFXN3 in human leukemic cells. However, the
131 defect in purine synthesis is rescued only by SFXN2, SFXN3, *dSfxn1* and *S. cerevisiae* FSF1 [8]. Thus,
132 most SFXN appear functionally redundant in serine import although probably with different kinetic
133 properties. Moreover, they might also ensure the mitochondrial import of other metabolites.

134 3.2 Sideroflexins in central carbon metabolism

135 Disturbance of central carbon metabolism was reported in SFXN1-null cells. A LC-MS analysis
136 of tricarbohylic acid (TCA) cycle metabolites contained in HEK *SFXN1* KO cells showed significantly
137 reduced levels of citrate and isocitrate while α -ketoglutarate (α -KG) was decreased and succinate
138 cellular levels were unchanged [15]. Isotopic labelling experiments helped understanding the role of
139 SFXN1 in mitochondrial metabolism. ^{13}C metabolic flux analysis (^{13}C MFA) is a useful tool to assess
140 intracellular fluxes and get clues on the metabolic pathways that are differentially activated in
141 mammalian cells depending of the genetic context or environmental conditions [48]. Using ^{13}C MFA
142 to investigate metabolic fluxes in HEK *SFXN1* KO cells, Acoba *et al* provided evidence for a reduced
143 activity of the glutamate dehydrogenase (GDH) that converts Glu in α -KG using NAD(P)⁺ as a
144 coenzyme [49,50]. The lower activity of GDH is unlikely due to a lowering in NAD(P)⁺ since
145 NAD(P)⁺/NADPH ratio was unchanged in SFXN1-deficient cells [15]. In animals, GDH is regulated
146 by a wide variety of ligands (NADH, GTP, ATP, palmitoyl-coA, steroid hormones, leucine) and the
147 mitochondrial enzymes SIRT4 and SCHAD. Alanine aminotransferase (ALT) activity is also
148 markedly reduced in SFXN1-null cells [15]. This deficiency in alanine catabolism is probably due to
149 the lower availability of α -KG in SFXN1-null cells. Alanine aminotransferase (also known as GPT) is
150 implicated in L-alanine degradation via transaminase pathway and uses pyridoxal 5'-phosphate as a
151 cofactor. A comprehensive review of nitrogen utilization and amino acid metabolism can be found
152 in [51]. Mitochondrial levels of GDH and ALT2 (mitochondrial alanine aminotransferase) were not
153 investigated in SFXN1-deficient cells and we wonder if the absence of SFXN1 could trigger a decrease
154 in the mitochondrial import or stability of some mitochondrial enzymes intervening in the catabolism
155 of amino acids that fuel the TCA cycle. Acoba *et al* also performed ^{13}C MFA with [U- ^{13}C]-glucose to

156 fuel the TCA cycle with [U-¹³C]-labelled acetyl-coA and provided evidence for an increase in the
157 incorporation of glucose in the TCA cycle [15].

158 NAD⁺/NADH ratio was also increased in SFXN1 KO cells and, altogether, the results obtained
159 by Acoba *et al* shed light on a disturbance of central carbon metabolism upon the loss of SFXN1.
160 Whether the deficiency in SFXN1 orthologues and the other human sideroflexins also affects central
161 carbon metabolism is an open question that is not fully elucidated.

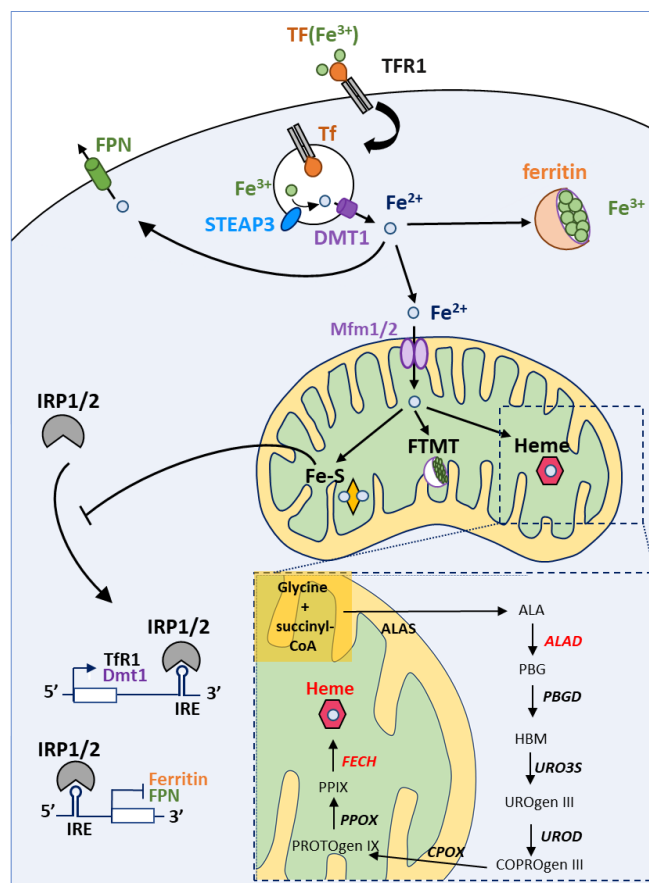
162 4. Sideroflexins, iron homeostasis and heme biosynthesis

163 4.1. A brief overview of iron homeostasis, ISCs and heme biosynthesis

164 Iron is an essential cofactor for several enzymes involved in redox reactions due to its ability to
165 exist in two ionic forms: ferrous iron (Fe²⁺) and ferric iron (Fe³⁺). Iron is thus easily oxidized and
166 reduced which makes it suitable for redox reactions. Thus, iron is a key player in many important
167 cellular processes, including energy metabolism, respiration and DNA synthesis. The implication of
168 iron in all these processes is done through the incorporation of this atom in complex structures
169 synthesized mainly in the mitochondria: iron-sulfur clusters and heme. Iron homeostasis is a tightly
170 controlled process in which numerous proteins intervene [52–55]. **Figure 4** depicts the main actors of
171 iron trafficking and metabolism at the cellular level.

172 Maintaining iron homeostasis is essential for cell viability and iron intracellular levels are thus
173 tightly controlled by Iron Regulatory Proteins (IRP1 / 2). IRP1/2 regulate the levels of key proteins
174 intervening in iron homeostasis by binding to Iron Responsive Element (IRE) sequences either located
175 in the 5'UTR or in the 3'UTR of mRNA encoding actors of iron metabolism. For example, when
176 cellular iron levels are low, IRP proteins bind to IRE in the 5' UTR of ferritin and ferroportin mRNAs
177 (among others) and thereby inhibit their translation. The IRPs proteins can also bind to IRE in the
178 3'UTR of iron-regulated mRNAs, such as TfR1 and DMT1 mRNAs encoding two proteins involved
179 in iron uptake, thereby preventing endonuclease-mediated degradation of these mRNAs (see [56] for
180 a review). Thus, this regulation by IRP proteins under low iron concentration leads to an increase in
181 iron uptake as well as a decrease in iron storage and export. On the opposite, under high iron levels,
182 the synthesis of iron-sulfur clusters is enhanced. The binding of an iron-sulfur cluster to the IRP1
183 protein leads a conformational change inhibiting its IRE binding activity but promoting its aconitase
184 activity. The ACO1 enzyme (*e.g.*, Fe-S bound IRP1) catalyzes the conversion of citrate and isocitrate
185 in the cytosol enhancing, probably, NADPH generation and lipid synthesis [57]. Our aim is not to
186 give an extensive review of the IRE-IRP signaling pathway and numerous comprehensive reviews
187 can be found elsewhere, such as in [58].

188 Iron-sulfur clusters are made up of iron and sulfur ions which come together to form [1Fe-0S],
189 [2Fe-2S], [3Fe-4S] and [4Fe-4S] clusters [59]. Fe-S clusters (ISCs) are found in numerous
190 metalloproteins such as aconitase 1 [54,60–62]. Thus, ISCs are involved in a wide variety of cellular
191 processes among which we can cite the Krebs cycle, mitochondrial respiration, DNA replication /
192 repair. Assembly of the Fe-S center is carried out by the ISC machinery. Inorganic sulfur is first
193 produced from the cysteine by the cysteine desulfurase NFS1. Then, the Fe-S cluster is formed on the
194 ISC assembly enzyme (ISCU) with the help of frataxin (FXN) [63].



195

196 **Figure 4. Iron homeostasis and utilization at the cell level.** Iron cellular uptake is controlled by
 197 transferrin and its receptor (Tf and TFR1, respectively). Afterwards, in the endosome, iron is reduced
 198 thanks to the action of STEAP3 (which converts the insoluble Fe³⁺ to soluble Fe²⁺) and released from
 199 the endosome into the cytoplasm by the DMT1 channel. Free iron can be stored by ferritin in the
 200 cytoplasm or can be transported into the mitochondria, thanks to Mitoferrin 1 and 2 transporters
 201 (Mfrn1/2). Excess of iron is released out of the cell by Ferroportin (FPN). Inside the mitochondrion,
 202 iron can be stored in FTMT (mitochondrial ferritin) or incorporated in heme or Fe-S clusters. IRP1 and
 203 2 (Iron Related Protein 1 and 2) are the major regulators of iron metabolism. In iron-depleted cells,
 204 IRP1 can bind IRE (Iron Response Elements) motifs to promote or repress mRNA translation. If IREs
 205 are located in the 5'UTR, IRP1 binding represses mRNA translation under low iron levels. On the
 206 contrary, transcripts with IREs at the 3'UTR are stabilized and translated upon IRP binding. Hence,
 207 low iron levels lead to decreased Ferritin and FPN levels but promote TFR1 and DMT1 synthesis.
 208 High levels of iron prevent IRP1 binding to IREs (see main text for details).

209 Heme is a complex of ferrous iron and protoporphyrin IX (PPIX). It is an important prosthetic
 210 group for many vital proteins, such as hemoglobin, myoglobin, cytochromes and CYP450 proteins
 211 [64,65]. Heme is involved in the transport and storage of oxygen, the transfer of electrons for
 212 enzymatic redox reactions, signal transduction, ligand binding and control of gene expression [66].
 213 Heme biosynthesis (**Figures 4, 6**) is a pathway comprising eight steps, among which four arise inside
 214 the mitochondrion (*e.g.* the first and the last three steps). The rate limiting enzyme of this process is
 215 the ALA-synthase (ALAS) responsible for the synthesis of δ -aminolevulinic acid (ALA) from the
 216 condensation of glycine and succinyl-CoA, in the presence of pyridoxal-5'-phosphate [67,68]. Two
 217 genes encode ALA-synthases: *ALAS1* is the ubiquitously expressed one while *ALAS2* expression is
 218 restricted to erythroid cells. Negative feedback regulation of *ALAS1* by heme has been reported and
 219 will be discussed later. Ferrochelatase (FECH) catalyses the last step of heme biosynthesis, namely
 220 the insertion of iron into PPIX. Heme biosynthesis has been extensively reviewed elsewhere
 221 [52,55,69].

222 4.2. Can sideroflexins regulate iron homeostasis ?

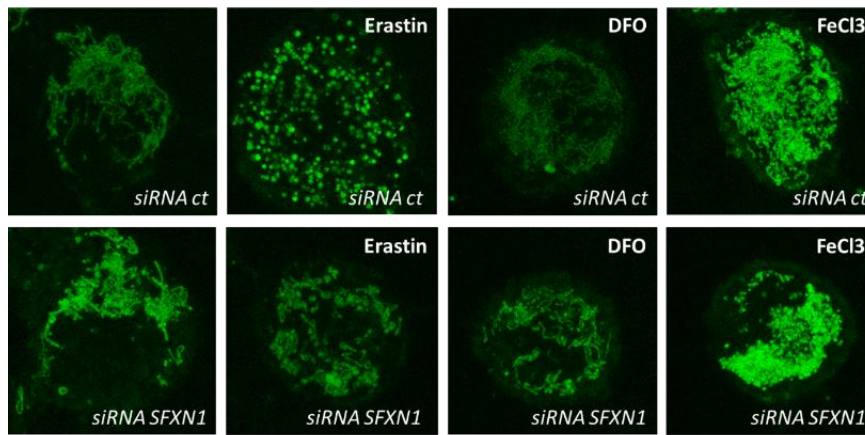
223 The first evidence for a link between sideroflexins and iron metabolism came from a study of
224 the *flexed-tail* mouse, which harbors a mutation in a locus containing the *Sfxn1* gene [1]. Mice mutant
225 for *Sfxn1* displayed sideroblastic anemia, microcytic anemia and hypochromic erythrocytes.
226 Furthermore, *flexed-tail* mice were also displaying iron deposits in the mitochondria from erythrocyte
227 precursors. Nevertheless, no mechanisms regarding the iron accumulation in the mitochondria were
228 proposed; but since then, sideroflexins were annotated as proteins implicated in iron metabolism.

229 Based on the annotation of SFXN as transporters of metabolites required for iron metabolism,
230 we and others have tried to monitor the consequences of the loss of SFXN on iron cellular levels.
231 **Table 3** summarizes the experimental evidence for an iron imbalance in the absence of SFXN.
232 Whereas Mon *et al.* reported increased mitochondrial iron levels in HEK SFXN2 KO cells [9], an ICP-
233 MS analysis did not show significantly modified cellular or mitochondrial iron levels in HEK *SFXN1*
234 KO cells compared to parental cells but an increase in cellular Mn^{2+} [15]. Of note, albeit not significant,
235 it seems that the loss of SFXN1 also slightly enhanced mitochondrial iron levels measured by ICP-
236 MS, with a more pronounced effect in one of the two SFXN1-KO clones [15]. Maybe, a significant
237 increase could have been seen with more replicates or by quantifying mitochondrial iron by a TEM-
238 EDX analysis as done for SFXN4 KO cells [31]. Despite an appropriate methodology, caution must
239 also be taken when analyzing the results obtained by Mon *et al* because this study was done with
240 only one cellular clone obtained after CRISPR/Cas9 invalidation of the *SFXN2* gene. However,
241 expression of a SFXN2-mCherry fusion protein restored basal mitochondrial Fe^{2+} levels in these
242 SFXN2 KO cells, as measured with a specific fluorescent probe. Loss of SFXN4 was also proven to
243 alter iron levels in the K562 leukemic human cell line. Whereas labile cytosolic iron pool was
244 decreased, Paul *et al.* have provided evidence for a redistribution of cellular iron from the cytosol to
245 the mitochondria in K562 *SFXN4* KO cells [31].

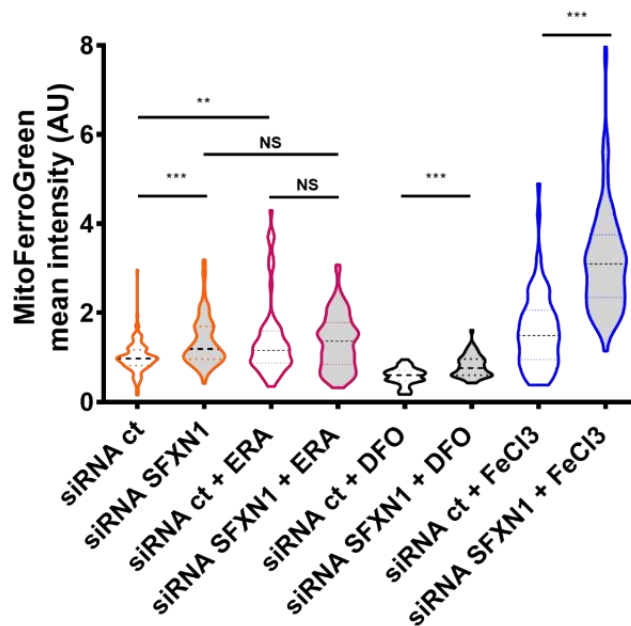
246 In our lab, we are interested in the early events triggered by the depletion of SFXN1 in
247 mammalian cells. To investigate the effect of a decrease in SFXN1 protein levels, we chose to
248 transiently deplete SFXN1 in HT1080 human cells using siRNA and then, we quantified
249 mitochondrial labile Fe(II) levels using the MitoFerro-Green probe [70]. Depleting SFXN1 in HT1080
250 cells induced a slight but reproducible increase in mitochondrial iron levels as shown in **Figure 5**.
251 This increase in mitochondrial Fe(II) when SFXN1 levels are lowered, could be either a consequence
252 of a defective heme biosynthesis, since Fe(II) is the substrate of FECH that inserts it into
253 protoporphyrin IX, or a consequence of the catabolism of heme by HO-1 (heme oxygenase-1).
254 Additionally, our data enlighten an erastin-dependent increase in labile Fe(II) mitochondrial levels
255 in HT1080 cells. A similar increase was also reported in erastin-treated MEF cells [71]. In HT1080 and
256 MEF cells, erastin was previously shown to induce HO-1 expression [72,71], which may explain the
257 increase in mitochondrial Fe(II) that we observed in erastin-treated H1080 cells. Whether reducing
258 SFXN1 levels inhibits FECH activity or promotes heme catabolism must be further investigated.

259 Altogether, the evidence enounced above point towards a role for SFXN in the maintenance of
260 appropriate iron levels since the depletion or loss of SFXN1, SFXN2 and SFXN4 may increase
261 mitochondrial iron by mechanisms that remain unknown. Mitoferrin1 and Mitoferrin2 are known as
262 iron importers into the mitochondria and ABCB8 as an iron exporter [73]. Thus, due to the fact that
263 iron mitochondrial transporters have been already described, and that the lack of either SFXN 1, 2 or
264 4 leads to intramitochondrial iron accumulation, we do not favor the possibility that SFXN are iron
265 transporters. So, other intriguing possibilities should be explored.

266



Mitochondrial Iron Accumulation



267

268

269

270

271

272

273

274

275

276

277

278

279

280

281

282

283

284

Figure 5: Depleting SFXN1 in HT1080 human cells leads to an intramitochondrial iron accumulation. *Top panel:* mitochondrial labile Fe(II) staining using the MitoFerro-Green probe [70] after transient transfection with a control siRNA (siRNA ct) or a pool of SFXN1-targeting siRNA (siRNA SFXN1). Cells were further treated with DMSO (vehicle), erastin, DFO or FeCl₃. Erastin is a drug that is widely used to trigger ferroptosis, DFO (deferroxamine) is an iron chelator that lowers mitochondrial iron levels and is used as a negative control. FeCl₃ increases intracellular iron levels and served as a positive control. SFXN1 depleted cells show higher mitochondrial iron levels than control cells (siRNA scramble transfected cells). Erastin promotes iron accumulation. In control cells (siRNA ct), erastin increases mitochondrial iron levels and a punctuate staining is seen, maybe revealing mitochondrial network fission. In SFXN1 depleted cells, erastin does not seem to further increase mitochondrial iron levels. In all conditions except with erastin, iron levels are increased after SFXN1 depletion, compared to control, suggesting that erastin and SFXN1 could use the same mechanisms to lead to an increase in mitochondrial iron. Same magnification is used for all images. *Bottom panel:* quantification of three independent assays (n>50 cells per condition) in which fluorescent signal is measured and values are normalized to siRNA ct mean levels (mean =1). After Mann-Whittney tests, significant differences are shown (** p<0.01, *** p<0.001, NS Not Significant). See Appendix A.2 for experimental details.

285

286

287 Proper iron homeostasis requires a fluid transport of iron and its derivatives through the
288 mitochondrial membranes and the cytosol. In this regard, the ALA (Aminolevulinic acid) synthesis
289 requires Gly import through SCL25A38 on the one hand, and ALA export on the other hand,
290 presumably through the same transporter (**Figure 6**) [74]. SFXN1 was shown to be a Serine
291 transporter *in vivo* [8]. Intramitochondrial Ser would be catabolized by SHMT2 into Gly and 5,10-
292 meTHF (5,10 methyl tetrahydrofolate) to enter in the OCM pathway, necessary for purine synthesis,
293 pointing out that SFXN1 could be linked to the first and limiting step of heme synthesis. Moreover,
294 once protoporphyrin is generated in the intermembrane space, it must enter the mitochondrial matrix
295 for the last heme synthesis step using both ABCB6 and ABCB10 transporters [75,76]. Anyway, it
296 cannot be excluded that other sideroflexins could be involved in this event. Whether SFXN1 could
297 bind to heme and help in its trafficking is another hypothesis that merits our attention. We thus seek
298 for heme binding motifs (HBMs) in SFXN1 with the SeqD-HBM tool dedicated to the prediction of
299 heme-coordination sites in protein sequences [77,78] and we found four HBMs that are solvent-
300 accessible (**Figure S1, Appendix A**). These predicted HBM may permit transient interactions between
301 heme and SFXN1. Biochemical studies are needed to confirmed these interactions and further
302 investigate their significance regarding SFXN1 activity.

303 To conclude, several open questions are remaining about the role of SFXNs in iron homeostasis.
304 For example, are SFXN3 and SFXN5, like SFXN1, 2 and 4, able to regulate iron levels? No studies
305 have been performed in this regard yet. Do sideroflexins alter iron levels by regulating the activity of
306 other regulators implicated in iron homeostasis? How can we explain that low SFXN1 levels (as well
307 as low levels of SFXN2 or 4) lead to an increase of mitochondrial iron, and that an increase in SFXN1
308 may also trigger an increase mitochondrial iron level (see section 5.2)? What are the relationships
309 between iron homeostasis disturbance and one carbon metabolism? To answer those questions,
310 further work in mammalian cells is needed, and later confirmed using *in vivo* models.

311 4.3. Which role for sideroflexins in heme biosynthesis and ISC biosynthesis ?

312 Whether SFXN1 and its homologues can regulate heme biosynthesis has not been thoroughly
313 investigated so far, but recent studies gave evidence for an impairment of heme biosynthesis when
314 certain members of the SFXN family are lacking [9,15,31]. Interestingly, SFXN1 loss in human kidney
315 embryonic cells was recently reported to impair heme biosynthesis [15]. Indeed, cells lacking SFXN1
316 showed reduced heme levels, decreased CPOX and FECH transcripts and protein levels but increased
317 ALAS1 protein levels. It is well-known that heme can induce ALAS1 degradation by a mechanism
318 involving, at least, ALAS1 binding to the mitochondrial protease CplXP [79]. It is thus likely that low
319 heme levels found in SFXN1 cells limits heme binding to ALAS1 and consequently inhibits its
320 degradation by CplXP. These defects in heme biosynthesis may explain the less efficient
321 mitochondrial respiration and, especially, Complex III loss of activity. Accordingly, whereas formate
322 had no effect, hemin supplementation increased CIII activity in wild-type and *SFXN1* KO cells but
323 only partially restored the assembly of CIII in *SFXN1* KO cells [15]. However, hemin was unable to
324 restore basal levels of Complex III subunits in HEK *SFXN1* KO cells suggesting that other defects are
325 present in these cells. Interestingly, DMK (dimethyl- α -KG, a cell permeant analogue of α -KG)
326 rescued almost totally CIII subunits levels and CIII activity in HEK *SFXN1* KO. Succinyl-coA that
327 serves in the first step of heme biosynthesis can originate from α -KG or succinate. Hence, in the
328 mitochondrial matrix, α -KG can be converted in succinyl-coA by α -KG dehydrogenase, a highly
329 regulated enzyme of the TCA cycle [80]. It would thus be interesting to determine if, additionally to
330 the decreased GDH and ALT activity observed in *SFXN1* null cells [15], α -KGDH activity is also
331 impaired upon the loss of SFXN1.

332

333

334

Table 3. Regulation of systemic or cellular iron levels by SFXN

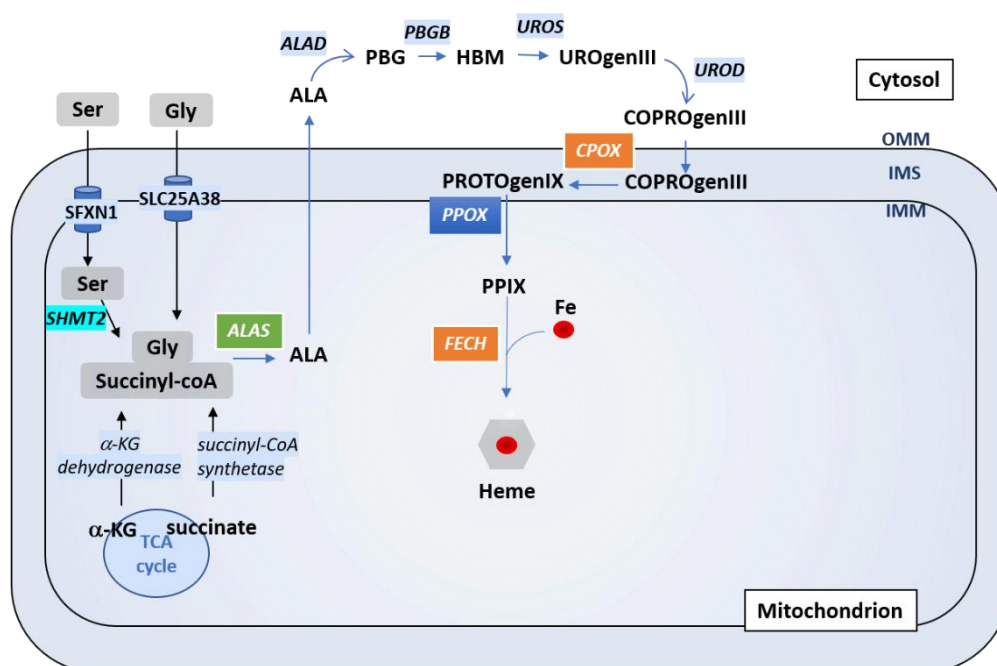
<i>Protein</i>	<i>Model</i>	<i>Evidence</i>	<i>Methodology</i>	<i>Reference</i>
<i>SFXN1</i>	Mouse	Iron overload in mitochondria of erythrocytes in the <i>flexed-tail</i> mouse	Iron mitochondrial staining	Fleming <i>et al</i> , 2001
<i>SFXN2</i>	HEK SFXN1 ^{KO} cells	Increased mitochondrial iron	ICP-MS	Acoba <i>et al</i> , 2020
	HEK SFXN2 ^{KO} cells	Increased mitochondrial iron levels	ICP-MS MitoFerro-Green staining and confocal microscopy	Mon <i>et al</i> , 2019
<i>SFXN3</i>	Mouse Sfnx3 KO	Decreased circulating iron levels in male transgenic mice homozygous for the Sfnx3 ^{tm1b(KOMP)Wtsi} allele	Biochemical assay	The IMPC database ²
<i>SFXN4</i>	K562 SFXN4 ^{KO} cells	Decreased labile iron pool	Indirect biochemical measure based on the dequenching of calcein upon release of iron	Paul <i>et al</i> , 2019
		Increased mitochondrial iron levels	TEM-EDX	
<i>SFXN5</i>	-	-	-	-

335

336

¹ ICP-MS is for inductively coupled plasma atomic emission - mass spectrometry, TEM-EDX is for Transmission electron microscopy-Energy dispersive X-Ray analysis. ² website page for SFXN3 : <https://www.mousephenotype.org/data/genes/MGI:2137679#phenotypesTab>

337 Impairment of heme biosynthesis upon SFXN loss could be explained by the function of serine
 338 transporter attributed to SFXN. Following its import into the mitochondrion, Ser can be converted in
 339 Gly and 5,10-me-THF involved in folate cycle and OCM. An imbalance in the cellular Ser/Gly ratio
 340 may impair heme biosynthesis since Gly is (with succinyl-coA) the precursor for the synthesis of
 341 protoporphyrins into which iron is incorporated in the final step of heme synthesis catalyzed by
 342 FECH (Figure 6). As SFXN1 is presumed to be the mitochondrial transporter of Ser, its loss could
 343 increase cellular Ser and lower Gly levels. Indeed, in Jurkat and K562 SFXN1 KO cells, the cellular
 344 Ser/Gly ratio was increased and associated to increased cellular Ser levels but decreased Gly levels
 345 [8]. In agreement with an imbalance in serine levels upon SFXN1 loss, HEK SFXN1 KO cells also have
 346 increased cellular Ser levels and Ser/Gly ratio but no decrease in Gly cellular levels were reported
 347 [15]. Whether this discrepancy can be explained by a cell type specificity or other reason remains to
 348 be elucidated. Of note, mitochondrial levels of those two amino acids have not been assessed and it
 349 will be interesting to more specifically address the presence of Ser and Gly inside the mitochondrion
 350 by a metabolomics study on this organelle.



351
 352 **Figure 6: Regulation of heme biosynthesis by SFXN1.** Gly and succinyl CoA are the substrates to
 353 generate ALA, the first heme precursor, thanks to ALAS enzyme. Gly can enter directly into the
 354 mitochondria by SLC25A38, or can be the result of Ser transformation (previously imported by
 355 SFXN1) by SHMT2. ALA is further exported to the cytosol where the next steps of heme biosynthesis
 356 are catalysed by ALAD, PBGB, UROS and UROD. CPOX, PPOX and FECH are the three
 357 mitochondrial enzymes that catalyze the three last steps of heme synthesis (see main text). The last
 358 step corresponds to the incorporation of iron into the protoporphyrin PPIX to complete the heme
 359 synthesis. Cells lacking SFXN1 show decreased CPOX and FECH mRNA and protein levels (orange
 360 box), but higher amount of ALAS protein (green box), according to Acoba *et al.* [15]

361 SFXN2 has been recently described in HEK293 cells to have a key role in iron metabolism, mainly
 362 in heme synthesis [9]. High levels of iron have been shown in mitochondria in SFXN2 knockout
 363 HEK293 cells. Also, a decreased activity of Complexes II-IV but not of the Complex I was noticed.
 364 Complex I subunits contain Fe-S clusters, in contrast to Complex IV, which is mainly composed by
 365 heme groups. Complexes II and III contain both Fe-S clusters and heme groups (Figure 2). Thus, as
 366 no effect in Complex I was detected, and no decrease in Frataxin (FXN), a mitochondrial enzyme
 367 required for the Fe-S cluster formation, nor in ALAS2, the enzyme that catalyzes the first step of the
 368 heme biosynthetic pathway, was reported, it was concluded that SFXN2 mutants affected heme
 369 synthesis after the first step of heme biosynthesis, but not the Fe-S cluster formation. However,

370 neither the levels of ISC-containing proteins nor those of ALAS1 have been assessed in this study. It
371 is surprising because ALAS2 is the erythroid specific form and ALAS1 the housekeeping one.

372 We propose few possibilities to explain *SFXN2* knockout cells phenotype. The lack of *SFXN2*
373 could either lead to an impaired ALA export or no mitochondrial import of protoporphyrin (PPIX)
374 for the last step of the heme pathway. A defective mitochondrial export of the heme groups is another
375 plausible explanation. Finally, other options could be possible as an interaction of *SFXN2* with *BCS1L*,
376 a chaperone anchored to the inner mitochondrial membrane that is required for proper assembly of
377 the Complex III (see section 2.2 for more details). In all those cases, an intramitochondrial iron
378 accumulation is presumed. All those possibilities, and others, must be studied to be able to clarify the
379 possible role of *Sfxn2* in heme biosynthesis.

380 4.4. Which role for sideroflexins in ISC biosynthesis ?

381 Loss of *SFXN* also seems to impair ISC biogenesis. Indeed, in the absence of *SFXN4* there is a
382 decrease in Fe-S cluster levels which is consistent with the decrease of Complex I activity seen in
383 *SFXN4* KO cells, pointing out that this *SLC56* carrier could play a role in Fe-S biosynthesis [30,31]. As
384 a consequence of the low Fe-S levels, *IRP1* aconitase activity, as well as labile iron cytosolic levels,
385 also decreases, whereas mitochondrial iron increases, suggesting that iron import in the mitochondria
386 is not impaired, and instead possibly enhanced. Those features are very similar to the lack of
387 mitochondrial frataxin, which leads to Friedreich's Ataxia, also known as X-linked sideroblastic
388 anemia. Frataxin (*FXN*) is a mitochondrial chaperone that interacts with aconitase in a citrate-
389 dependent manner to convert $(3\text{Fe-4S})_1^+$ inactive enzyme into $[4\text{Fe-4S}]_2^+$ active one within the Krebs
390 cycle. It also interacts with the *ISCU-NFS1* (Iron-Sulfur Cluster Scaffold-Cysteine desulfurase) in the
391 final steps of Fe-S formation [81,82]. The reduction of mitochondrial aconitase (*ACO2*) in *SFXN4* KO
392 cells [31] suggests that *SFXN4* could participate in the Fe-S biosynthesis maybe through an interaction
393 with Frataxin (*FXN*). It has been previously reported that *FECH*, an important enzyme for heme
394 biosynthesis, *Mfn1*, an iron transporter into the mitochondria, and *ABCB10*, a protoporphyrin IX
395 transporter, could form a complex in mouse erythroleukemia (MEL) cells to direct iron incorporation
396 into protoporphyrin to form heme [54,83]. Taken together, those results open the possibility that
397 *SFXN4* and *FXN* interact with other proteins such as aconitase or the *ISCU-NFS1* multimeric complex
398 to mature the Fe-S clusters. We have recently performed a screen with the aim to identify the direct
399 partners of *SFXN1* protein in MCF7 cells (Tifoun *et al.*, in preparation) and, even though *Sfxn1* does
400 not interact directly with *FXN*, it is still possible that *Sfxn4* could do so. In *Sfxn4* mutants Fe-S
401 synthesis is reduced, pointing out that *Sfxn4* may play a role in the first steps of Fe-S cluster
402 formation, maybe through *FXN* interaction. A recent study shows that the ISC (Iron Sulfur Cluster,
403 composed by *NFS1*, *ISCU* and *FXN*) function requires L-Cysteine to generate de disulfide groups
404 necessary to form the Fe-S clusters [84]. Moreover, it has been postulated that *SFXN1* could transport
405 not only serine, but alanine and possibly also glycine and cysteine *in vitro* [8]. Actually, in *SFXN1*
406 depleted cells have a proliferative advantage in media containing low cystine (dimer of cysteine
407 formed under oxidant conditions), this could be due to the fact that the amino acid cysteine is
408 necessary for cytosolic glutathione synthesis and that a loss of mitochondrial import would increase
409 its availability for those purposes [8]. The lack of *SFXN1* activity can be overcome by *SFXN2* and
410 *SFXN3* but not by *SFXN4* [8]. *SFXN4* cannot substitute *SFXN1* for Ser import into the mitochondria,
411 but it could maybe have a higher affinity for Cys. This may explain why *SFXN1* and *SFXN2* mutants
412 present mainly problems in heme synthesis whereas *SFXN4* KO cells have deficiencies in Fe-S cluster
413 formation, as Ser and Gly are essential for the ALA synthesis and Cys is required for proper Fe-S
414 maturation.

415 How could *SFXN* regulate iron levels and heme biosynthesis remains unanswered and whether
416 *SFXN* impair mitochondrial iron and heme homeostasis by direct or indirect actions is unknown. We
417 have recently documented the interaction between *SFXN1* and *ATAD-3* (Tifoun *et al.*, in preparation).
418 Because *Caenorhabditis elegans* *ATAD-3* was shown to modulate mitochondrial iron and heme
419 homeostasis, heme biosynthesis regulation by *SFXN1* may depend on its interaction with *ATAD-3*.
420 Interestingly in *atad-3* (RNAi) worms, mitochondrial but not cytosolic iron levels were increased and

421 an altered expression of iron homeostasis genes was reported [85]. Indeed *atad-3* knockdown (KD)
422 led to an increase in *ftn-1* but a decrease in *ftn-2* mRNA (respectively encoding the intestinal ferritin
423 heavy chain and a more ubiquitous one). *aco-1* (encoding the homologue of the mammalian IRP
424 responsible of the post-translational regulation of ferritin), *fpn-1.1* (encoding a *C. elegans* ferroportin
425 homologue) and *smf-3* mRNA (involved in the cellular uptake of non-heme iron) were reduced.
426 Expression of *mfn-1* (the sole Mitoferrin encoding gene in *C. elegans*) was unchanged upon *atad-3*
427 knockdown. In agreement with a mitochondrial iron overload, *atad-3* KD in worms also led to an
428 accumulation of Hemin (a heme-containing protein involved in erythroid differentiation) and a
429 fluorescent analogue of heme.

430 Interestingly, a new mutation of ATAD3A (Arg528Trp), which has been described in 7 families
431 [86], is responsible of developmental delay, hypotonia, optic atrophy, axonal neuropathy and
432 hypertrophic cardiomyopathy. In some of those individuals, a deficiency of complex III and citrate
433 synthase was detected. Those results look similar to the consequences of the lack of SFXN1 or SFXN4
434 proteins. ATAD3A, being a transmembrane protein that binds both external and internal
435 mitochondrial membranes, could interact with SFXN1 and/or SFXN4 to control iron metabolism.
436 Moreover, the use of *Drosophila* in this study, allowed to see that either lack of *bor* (*belphegor*, ATAD3A
437 homologue), either the expression of a R534W form, a variant of Arg528Trp human ATAD3A, in the
438 larval neuromuscular junctions (NMJ) promoted a decreased of mitochondrial content, aberrant
439 mitochondrial morphology and increased autophagy. Complementary, *bor* overexpression promoted
440 larger and elongated mitochondria in the NMJ. Whether SFXN family has a role in autophagy
441 remains completely unexplored and merits attention.

442 5. Sideroflexins, ferroptosis and ferritinophagy

443 5.1 SFXN, cell death and ferroptosis

444 Growing evidence support the key role of iron metabolism in ferroptosis, even if the exact
445 mechanisms are not fully elucidated [87]. Ferroptosis is a physiological cell death contributing to
446 tissue homeostasis and implicated in pathology (cancer, neurodegenerative disease and cardiac
447 injury). Mechanistically, ferroptosis is an iron-dependent but caspase-independent regulated cell
448 death (RCD) triggered by uncontrolled lipid peroxidation leading to dramatic morphological changes
449 in mitochondria. For recent reviews on the place of mitochondria in ferroptosis regulation, the reader
450 is invited to refer to [88,89]. Ferroptosis can be triggered by diverse drugs such as erastin, RSL3 or
451 FIN56, among many others, and this type of RCD is prevented by iron chelators and antioxidants
452 [90]. The mitochondrion appears as a main contributor to ferroptosis because of its central place in
453 iron metabolism and the fact that several mitochondrial metabolic pathways – including TCA cycle,
454 and ETC - contribute to PL-PUFA (polyunsaturated fatty acid containing membrane phospholipids)
455 peroxidation.

456 Few data are available on the role of SFXN in cell death and ferroptosis regulation. *SFXN4* gene
457 knockout was reported to promote cell death of K562 human cells in galactose-containing medium,
458 together with an increase in caspase 3/7 activity [31]. Whether the loss of SFXN4 triggers ferroptosis
459 was not investigated to our knowledge. Interestingly, in HEK kidney embryonic cells, *SFXN2* gene
460 knockout seems to sensitize cells to erastin-induced cell death however, the underlying mechanisms
461 were not deeply investigated [9].

462 Recently, SFXN1 was showed to participate in LPS-induced ferroptosis in H9c2 cardiomyocytes,
463 a process depending of NCO4A-mediated ferritinophagy [91]. Li *et al* showed an LPS- and NCO4A-
464 dependent upregulation of SFXN1 and documented the role of SFXN1 in LPS-induced ferroptosis.
465 Briefly, in LPS-treated H9c2 cardiomyocytes cells, knockdown of SFXN1 increased cell viability,
466 restored intramitochondrial basal levels, inhibited mitochondrial ROS production, decreased lipid
467 peroxidation and levels of PTGS2 (also known as cyclooxygenase-2) and MDA. Collectively, these
468 data suggest that SFXN1 promotes LPS-induced ferroptosis, however the molecular mechanisms are
469 far from being clear. Li *et al* explained this role by SFXN implication in the iron mitochondrial import,
470 which has not been proven yet. Further work is thus needed to investigate the relationships between

471 SFXN1 and ferroptosis, and the precise mechanisms whereby SFXN1 could regulate iron levels and
472 cell death. It will be also interesting to determine if SFXN1 mediates LPS-induced ferroptosis in other
473 cell types, as well as its implication in ferroptosis mediated by different inducers (such as erastin,
474 RSL3, FIN56 or other drugs). Because Acoba *et al.* reported lowered CoQ levels in SFXN1 KO cells
475 and CoQ is an antioxidant and a cofactor for the ferroptosis suppressor FSP1 [92], we expect that an
476 imbalance in SFXN1 levels may favor ferroptosis through a direct or indirect regulation of CoQ levels.
477 It would thus be interesting to study FSP1 activity in SFXN1 KO cells.

478 5.2. SFXN1 and ferritinophagy

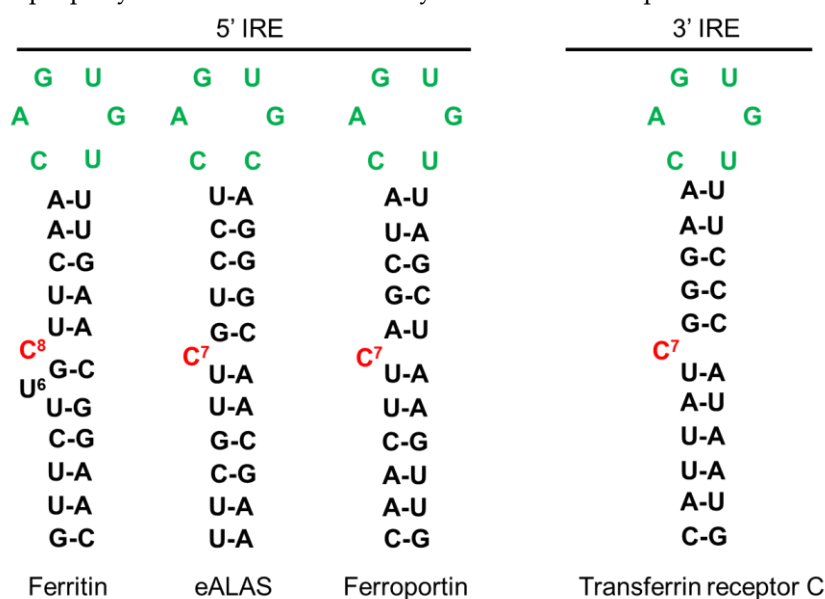
479 To limit the toxicity of free Fe²⁺, molecular traps – e.g. Ferritin and FtMt (mitochondrial ferritin) -
480 exist in the cytosol and the mitochondrion respectively, as stated earlier. Ferritinophagy, the
481 lysosome-dependent mechanism whereby iron is mobilized from ferritin, can also contribute to
482 ferroptosis induction. In this process, the selective cargo receptor NCOA4 (nuclear receptor
483 coactivator 4A) binds to ferritin and targets this iron storage protein to the lysosomes, thus promoting
484 ferritin degradation and the subsequent release of iron [93]. In apelin-13 induced cardiomyocytes
485 hypertrophy, Tang *et al* recently reported a decrease in FTH (ferritin heavy chain) together with an
486 upregulation of NCOA4 and SFXN1 [94]. Immunohistochemical analysis of hypertrophic heart tissue
487 also highlighted an upregulation of NCOA4 and SFXN1. The siRNA-mediated depletion of NCOA4
488 restored basal levels of SFXN1 in cardiomyocytes, suggesting that apelin-13 mediated upregulation
489 of SFXN1 could depend on NCOA4. In the presence of apelin-13, the knockdown of SFXN1 decreased
490 iron overload and mitochondrial ROS production in ferric ammonium citrate – treated
491 cardiomyocytes. How NCOA4 could upregulate SFXN1 remains unanswered, as well as the role of
492 SFXN1 and the other SFXN/SLC56 transporters in cardiac hypertrophy. In this study, SFXN1 is
493 proposed to be an iron importer, together with mitoferrin 1 and 2, which are upregulated. The
494 increase of mitochondrial iron in the induced cardiomyocytes hypertrophy model responds to the
495 elevated SFXN1 levels, and higher amounts of iron would promote ROS production thanks to the
496 Fenton reaction, an increase of lipids peroxidation and finally, an induction of ferroptosis.
497 Nevertheless, the mechanisms that allow SFXN1 to control iron levels are not addressed nor whether
498 SFXN1 is the most important player in regulating mitochondrial iron, aside of mitoferrins and
499 ferritin, is discussed.

500 NCOA4 mediated regulation of SFXN1 was also reported in a recent study addressing the role
501 of ferritinophagy in sepsis-induced cardiac injury [91]. In this study, SFXN1 was shown to be
502 upregulated at the mRNA level in LPS-treated cardiomyocytes, but whether this upregulation results
503 from a transcriptional activation or an enhanced stability of mRNA was not studied. To date, the
504 regulation of SFXN expression has not been deeply investigated and further work is needed to
505 document this point. However, intracellular iron may be important for NCOA4-mediated SFXN1
506 regulation since the iron chelator deferoxamine (DFO) was shown to decrease LPS-induced SFXN1
507 accumulation [91]. Li *et al* used immunofluorescence to show this DFO-mediated downregulation of
508 SFXN1 and this must be confirmed using western blot.

509 The iron-mediated regulation of SFXN1 levels is intriguing and we wondered if iron could
510 regulate translation or mRNA stability by IRP-dependent molecular mechanisms. We hypothesize
511 that IRP proteins, that are major regulators of iron homeostasis acting at the post-transcriptional
512 levels, could modulate SFXN levels through binding to cis-regulatory IRE response elements in
513 SFXN1 transcripts. We thus searched for IRP-binding sites in SFXN transcripts. IRE found in some of
514 the iron-regulated transcripts are shown in **Figure 7**. Canonical IRE are motifs composed of a six-
515 nucleotide apical loop (5'-CAGWGH-3') [95]. Using an IRE prediction tool ("SIREs Web Server 2.0"
516 (<http://ccbg.imppc.org/sires/>) [96], we retrieved putative IRE in all human SFXN1 variant transcripts
517 except for one (**Table 4**). One IRE of high quality and a second one of low quality are found
518 respectively at the end of the SFXN1 coding sequence and in the 3' UTR (**Figure 8**). Additionally,
519 human SFXN2 transcripts possess one putative medium-quality IRE and SFXN5 transcripts contain
520 a putative high-quality IRE, at their 3' UTR. Interestingly, no IREs are predicted neither in SFXN3 nor
521 in SFXN4 mRNAs. As SFXN1 and SFXN3 are closely related and seem to have highly similar three-

522 dimensional structure, it is tempting to hypothesize that they can be differentially regulated
 523 depending on iron levels. In *Drosophila*, no putative IREs are predicted in any of the two mRNAs
 524 encoding dSfxn1/3 and dSfxn2, the SFXN orthologues found in flies. The presence of putative IREs
 525 at the 3'UTR of some of SFXN transcripts is suggestive of their IRP-mediated stabilization. We thus
 526 expect an increase of SFXN1 levels under low iron levels, when IRP1 lacks its Fe-S cluster and IRP2
 527 is degraded. This latter is not in agreement with the DFO-mediated downregulation of SFXN1 levels
 528 reported by Li *et al* [91]. IRE motifs found in SFXN transcripts are non-canonical IRE motifs derived
 529 from IRE sequences identified in IRP-interacting mRNAs uncovered in the genome-wide SELEX
 530 experiments [97–99]. Having found IRE in SFXN1 transcripts is in favor of an iron-mediated
 531 regulation of SFXN levels, however, whether the IREs found in SFXN1, SFXN2 and SFXN5 transcripts
 532 are functional, is a point that needs to be further investigated.

533 To conclude, despite two works started to shed light on SFXN1 role in iron homeostasis and
 534 ferroptosis [94,91], how this metabolite transporter exerts its function is far from being clear and more
 535 work is required to properly elucidate mechanistically how SFXN1 is implicated in iron homeostasis.



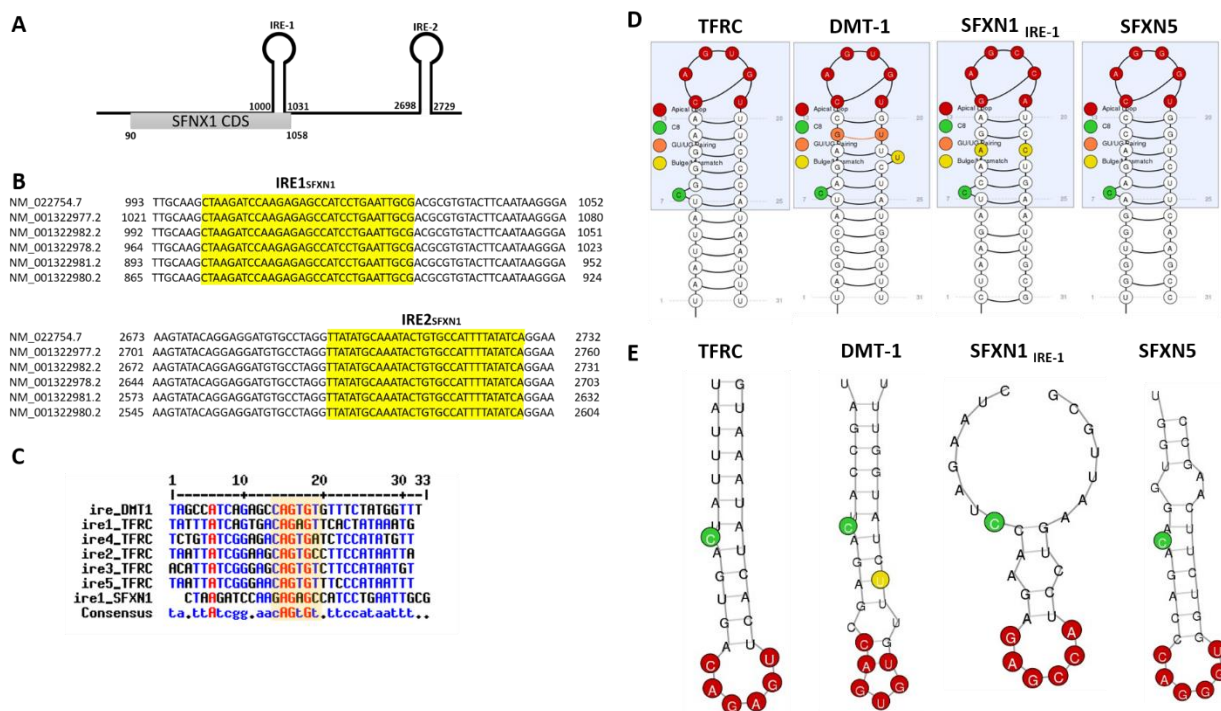
536 **Figure 7. IRE sequences from known proteins involved in iron metabolism.** IRE sequences can be
 537 localized at 5' or 3'. In the absence of iron, IRP1 binds the sequences located at 5' of blocking the translation of
 538 the RNA. Ferritin, ALAS and Ferroportin are proteins involved in iron storage, heme synthesis and iron export,
 539 respectively. In the same situation, IRP binding to 3' sequences, stabilizes the RNA promoting the translation of,
 540 for example, Transferrin receptor, involved in iron import. In the opposite situation, with high iron levels, IRP
 541 binds to iron, which unbinds the IREs, thus promoting translation of Ferritin, ALAS and Ferroportin and leading
 542 to Transferrin receptor RNA decay, which is no more protected by IRP1.
 543

544

545

Table 4. Location of predicted IRE in SFXN1 splicing variants

Sequence ID	mRNA length	CDS position	Product	IRE position
NM_022754.7 Homo sapiens sideroflexin 1 (SFXN1), transcript variant 1, mRNA	4066	90-1058	sideroflexin-1 isoform 1	1000-1031 2698-2729
NM_001322977.2 Homo sapiens sideroflexin 1 (SFXN1), transcript variant 2, mRNA	4094	118-1086	sideroflexin-1 isoform 1	1028-1059 2726-2757
NM_001322978.2 Homo sapiens sideroflexin 1 (SFXN1), transcript variant 3, mRNA	4037	244-1029	sideroflexin-1 isoform 2	971-1002 2669-2700
NM_001322980.2 Homo sapiens sideroflexin 1 (SFXN1), transcript variant 4, mRNA	3938	90-875	sideroflexin-1 isoform 4	872-903 2570-2601
NM_001322981.2 Homo sapiens sideroflexin 1 (SFXN1), transcript variant 5, mRNA	3966	118-903	sideroflexin-1 isoform 4	900-931 2598-2629
NM_001322982.2 Homo sapiens sideroflexin 1 (SFXN1), transcript variant 6, mRNA	4065	272-1057	sideroflexin-1 isoform 2	999-1030 2697-2728
NM_001322983.2 Homo sapiens sideroflexin 1 (SFXN1), transcript variant 7, mRNA	959	90-818	sideroflexin-1 isoform 3	No IRE

547
548

549 **Figure 8. Predicted IRE in SFXN transcripts.** A. Two IREs were found in the 3'UTR of SFXN1 transcripts
 550 using the SIREs Web Server 2.0. The first one is located at the end of the coding sequence. B. Alignment showing
 551 the position of the two IREs in SFXN1 transcripts. All except one shorter SFXN1 transcript variant possess
 552 putative IREs. C. Alignment of the IREs of DMT-1, transferrin receptor (TFRC) and SFXN1 transcripts using
 553 MultiAlin. The consensus highlights the position of the six-nucleotide apical loop (5'-CAGWGH-3') as shown in
 554 the yellow box. D, E. Schemes (D) and RNA fold prediction (E) for the IREs from TFRC, DMT-1, SFXN1 and
 555 SFXN5 transcripts generated by the SIREs Web Server 2.0.

556 6. Sideroflexins in aging: may SFXN regulate neuronal physiology and retinal function?

557 In this part, we discuss the potential role of SFXN in neuronal pathophysiology, aging and
 558 retinal function.

559 6.1. Sideroflexins and biometals in neuronal physiopathology

560 Brain accumulation of biometals - including iron and manganese - has been observed in
 561 neurodegenerative diseases and associated with a decline in cognitive functions [100–102].
 562 Accumulation of biometals can be detrimental and may promote protein aggregation. Hence,
 563 Amyloid beta peptide (A β), which forms toxic aggregates in the brain of patients who suffered from
 564 Alzheimer's disease, is known to interact with iron [103–106]. A β toxicity was reported to be
 565 suppressed by the iron storage protein Ferritin in *Drosophila* [107].

566 We postulate that some SFXN may share a neuroprotective role because SFXN are present in
 567 brain neurons (Human Protein Atlas, [27] and our unpublished data) and a decreased expression of
 568 SFXN1 and SFXN3 was linked to Alzheimer's and Parkinson's diseases (AD and PD). Indeed, SFXN1
 569 is decreased in brains of AD patients [108] and SFXN3 downregulated in late stage PD dopamine
 570 neurons from *substantia nigra* [109]. Additionally, downregulation of the *Drosophila* orthologue
 571 dSfxn1/3 enhanced tau toxicity in a *Drosophila* model commonly used to study neurodegeneration
 572 [108]. Under physiological conditions, SFXN3 and alpha-synuclein (α -Syn, a PD marker protein)
 573 levels were inversely correlated in a murine model, whereas overexpressing dSfxn1/3 impaired
 574 synapse morphology at the *Drosophila* neuromuscular junction [45]. It is tempting to link a putative
 575 iron-dependent regulation of SFXN, as discussed above, and the known regulation of α -Syn by IRPs.
 576 Hence, an IRE is found in the 5'UTR of α -Syn mRNAs and IRP-mediated translational inhibition is

577 relieved upon high iron levels [58,110]. This could explain the opposite regulation of α -Syn and SFXN
578 levels. However, we did not find putative IRE in SFXN3 transcripts, as stated above.

579 Decreased levels of SFXN1 in the hippocampus were also observed in a rat model with bilateral
580 ovariectomy displaying depressive behaviors and cognitive impairment [111]. Recent evidence point
581 towards a regulatory role for SFXN in iron homeostasis / utilization at the cell level [9,112,15].
582 However, iron homeostasis and heme biosynthesis have not been investigated specifically in SFXN-
583 deficient neurons yet, and it would be interesting to question this point. Besides the mitochondrial
584 accumulation of iron reported when some SFXN are lacking, Acoba *et al* also reported a decrease in
585 manganese levels in SFXN1-null cells [15]. Manganese is an essential metal element required for the
586 activity of certain enzymes (such as MnSOD) and both insufficiency and overexposure can affect
587 neuronal physiology and cognitive functions [113]. Thus, SFXN might regulate neuronal physiology
588 in participating in biometals homeostasis.

589 Whether SFXN are able to regulate ferroptosis is also an important concern, because ferroptosis
590 is one of the most important regulated cell death in brain [114]. Ferroptosis was reported in
591 Parkinson's disease, Alzheimer's disease and Huntington's disease and other neurologic disorders.
592 Using *in vitro*, *ex vivo* and *in vivo* (mouse) PD models, Do Van *et al.* [115] reported ferroptosis in PD
593 dopaminergic neurons, a process that was reversed by Ferrostatin-1, a selective inhibitor of erastin-
594 induced ferroptosis which inhibits lipid ROS. Growing evidence also highlight the implication of
595 ferroptosis in Alzheimer's disease [116], a neurodegenerative disease characterized by cognitive
596 functions and memory impairment, synaptic loss and neuronal cell death. In mouse, conditional
597 deletion in forebrain neurons of glutathione peroxidase 4 (Gpx4) gene altered cognitive functions
598 (spatial learning and memory) and triggered hippocampal neurodegeneration with hallmarks of
599 ferroptosis [117].

600 To conclude, further investigations must be undertaken to precisely specify the role of SFXN1
601 and its homologues in brain biometals homeostasis and neurodegeneration.

602 6.2. *Sfxn* and retinal degeneration

603 Iron levels vary during retina development, with gender and it accumulates during aging. When
604 supply does not equal demand (*e.g.* if retinal blood flow is impaired), retinal neurons are at risk of
605 excitotoxic cell death and vision is impaired or lost [118,119].

606 Many proteins are involved in iron homeostasis in the retina, and most of the rodent models
607 studied, are related to human pathologies, like human atransferrinemia (lack of transferrin),
608 hemochromatosis type IV (lack of ferroportin) or microcytic hypochromic anemia with iron overload
609 (decrease in DMT1), among others (see [119] for a review). Human transferrin electrotransfection in
610 rodents was shown to protect retinal structure and function, reducing microglial infiltration and
611 preserving the integrity of the outer retinal barrier in a photo-oxidative model. Transferrin, a natural
612 iron chelator, delayed also the retina degeneration and decreased oxidative stress [120]. This work
613 validates iron overload as a therapeutic target for pathologies as retinitis pigmentosa or age-related
614 macular degeneration. Taking into account the relationships between SFXN and iron metabolism, we
615 expect that the loss of SFXN could impair retinal function. Accordingly, in mice, *Sfxn3* mutations lead
616 to retinal degeneration [121]. Using forward genetics and screening by optical coherence
617 tomography, Chen *et al.* identified the *pew* and *basilica* mutations in the *Sfxn3* gene leading to a
618 significant decrease in the outer retina thickness. Mice with CRISPR-Cas9-induced *Sfxn3* loss-of-
619 function mutations were further generated to investigate the consequences on retinal structure and
620 function. Mice with predicted dramatically shortened *Sfxn3* proteins showed retinal impaired
621 morphology (decreased retinal thickness, especially that of the outer retina, and loss of the hexagonal
622 shape of retinal pigmentary epithelium cells) and abnormal fundus and vasculature compared to
623 controls. Retinal thickness even decreased with age in favor of a retinal degeneration due to the lack
624 of functional *Sfxn3*. Whether those defects are associated to impairment in iron homeostasis is not
625 explored nor discussed. Anyway, we favor the idea that SFXN3 contributes to regulate intracellular
626 iron levels, thus protecting the retina from oxidative stress. Moreover, in humans, SFXN4 loss-of-

627 function is associated with optic atrophy [19,21], pointing to SFXNs as a central family of proteins
628 required for proper retina development and homeostasis.

629 7. Conclusion and open questions

630 SFXN/SLC56 is a new family of mitochondrial proteins that have important roles in amino acid
631 transport and in iron homeostasis. Several studies associate SFXN depletion with an increase in
632 mitochondrial iron, deficiencies in carbon metabolism and RC activity and ferroptosis, in cell culture,
633 in animal models and in human pathology, making the SFXN an interesting target for tissue
634 degeneration therapy. But even though those links seem clear and reproducible, nothing is known
635 about the mechanism of action of SFXN. Do all the isoforms have the same functions (different
636 members are expressed in different tissues)? As there are several transcripts for each isoform, do
637 those different transcripts generate different proteins with different kinetic properties? If SFXN are
638 not iron transporters, how can they control iron levels in the mitochondria? How can they control
639 mRNA and/or protein levels of some key heme regulators (CPOX, FECH and ALAS)? Some SFXN
640 present putative IRE but other don't; are all SFXN sensible to iron content and to IRP1/2 regulation?

641 We think that a better knowledge on SFXN biochemistry is needed to properly decipher the
642 functions of each SFXN member, to know whether they all have redundant functions, their
643 interaction with other proteins or with other SFXN, and how they are regulated.
644

645 Abbreviations

646 ABCB6: ATP Binding Cassette Subfamily B Member, ACO1: Aconitase1, AD: Alzheimer's disease, α -KG: α -ketoglutarate, α -
647 KGDH: α -ketoglutarate deshydrogenase, AGK2 AcylGlycerol Kinase, ALA: Aminolevulinic acid, ALAD:
648 Aminolevulinic acid deshydratase, ALAS: Aminolevulinic acid synthase, ALT2: Alanine aminotransferase 2, ICP-MS:
649 Inductively coupled mass spectrometry, a-Syn: Alpha-synuclein, ATAD-3: ATPase family 3A domain containing protein,
650 A β : Amyloid beta peptide, BBG-TCC: Brain Bergmann Glial cell- Tricarboxylate carrier, BCS1L: Ubiquinol-Cytochrome C
651 Reductase Complex Chaperone, BMP: Bone Morphogenetic Protein, CCHL: Cytochrome c heme lyase, COPROgenIII:
652 Coproporphyrinogen III, CoQ: Coenzyme Q, COX4: Cytochrome c oxidase subunit 4, COXPD18: Combined oxidative
653 phosphorylation deficiency 18, CPOX: Coproporphyrinogen oxidase, CYP450: Cytochrome P450, Cyt b: Cytochrome b, Cyt
654 c1: Cytochrome c1, DFO: Deferoxamine, DMK: dimethyl- α -ketoglutarate, DMSO: Dimethyl sulfoxide, DMT1: Divalent metal
655 transporter 1, dSfxn: Drosophila sideroflexin, ETC: Electron transport chain, Fe²⁺: Iron ferrous, Fe³⁺: Iron ferric, Fe-S: Iron-
656 sulfur, FECH: Ferrochelatase, FeSFA: Fluorescence assay, FIN56: ferroptosis inducing 56, FLVCR1b: Feline leukemia virus
657 subgroup C receptor 1, Fp: Flavoprotein, fpn-1.1: Ferroportin 1.1, Fsl1: Fungal sideroflexin 1, FtMt: Ferritin Mitochondrial,
658 FXN: Frataxin, GDH: Glutamate dehydrogenase, Gpx4: Glutathione peroxidase 4, GTP: Guanosine Triphosphate, HBM:
659 Heme Binding Motif, HEK: Human embryonic kidney, HO-1: Heme oxygenase-1, ISCs: Iron-sulfur clusters, IMM: Inner
660 mitochondrial membrane, IMPC: International Mouse Phenotyping Consortium, IMS: Intermembrane space, IRE: Iron
661 Response Elements, IRP1/2: Iron Related Protein 1 and 2, ISCU: Iron-sulfur cluster assembly enzyme, ISP: Iron-sulfur protein,
662 LC-MS/MS: Liquid chromatography-coupled to tandem mass spectrometry ,LPS: Lipopolysaccharide, LYRM7: LYR motif-
663 containing protein 7, Madh5: Mothers against decapentaplegic homolog, MDA: Malondialdehyde, MEF: Mouse Embryonic
664 Fibroblasts, MEL: Mouse erythroleukemia, Mfrn1/2: Mitoferrin 1/2, MnSOD: Manganese superoxide dismutase, NAD(P)⁺ :
665 Nicotinamide adenine dinucleotide phosphate, NADH: Nicotinamide adenine dinucleotide hydrogen, NCO4A: nuclear
666 receptor coactivator 4, NDUFB8: NADH dehydrogenase [ubiquinone] 1 beta subcomplex subunit 8, NDUFS1: NADH
667 dehydrogenase (ubiquinone) Fe-S protein 1, NDUFS7: NADH dehydrogenase (ubiquinone) Fe-S protein 7, NDUFS8: NADH
668 dehydrogenase (ubiquinone) Fe-S protein 8, NDUFV1: NADH dehydrogenase [ubiquinone] flavoprotein 1, NFS1:
669 nitrogen fixation 1 homolog (S. cerevisiae), NMJ : Neuromuscular junctions, NUDFV2: NADH dehydrogenase [ubiquinone]
670 flavoprotein 2, OCM: One-carbon metabolism, OCR: Oxygen Consumption Rates, OXPHOS: Oxidative Phosphorylation, PD:
671 Parkinson's disease, PGB: Porphobilinogen, PL-PUFA: phospholipid-bound polyunsaturated fatty acids, PPIX:
672 Protoporphirin IX, PPOX: Protoporphyrinogen oxidase, PTGS2: Prostaglandin-Endoperoxide Synthase 2, RC: Respiratory
673 complexes , RCD : Regulated Cell death, RISP: Rieske iron-sulfur protein, ROS: Reactive oxygen species, RSL3: Ras-selective
674 lethality protein 3, SCHAD: Short-Chain 3-Hydroxyacyl-Coenzyme A, SDHA: Succinate dehydrogenase complex, subunit
675 A, SDHB: Succinate dehydrogenase complex, subunit B, SDHC: Succinate dehydrogenase complex, subunit C, Ser: Serine,
676 SFXN: Sideroflexins, SHMT2: Serine Hydroxymethyltransferase 2, SILAC: Stable isotope labeling by amino acids, SIRT4:
677 Sirtuin 4 , SLC25A38 Solute carrier Family 25 Member 38, SLC25A39: Solute Carrier Family 25 Member 39, SLC56: Solute

678 carrier family , STEAP3: Six-Transmembrane Epithelial Antigen of Prostate 3, STED: Stimulation Emission Depletion, TCA:
679 Tricarboxylic acid, TCC: Tricarboxylate carrier, TEM-EDX: Transmission electron microscopy linked with energy-dispersive
680 X-ray spectroscopy , TF: Transferrin, TFR1: Transferrin receptor protein 1, TIM22: Translocase of Inner Mitochondrial
681 Membrane 22, TTC19: Tetratricopeptide Repeat Domain 19, UQCC1-3: ubiquinol-cytochrome c reductase complex assembly
682 factor 1, UQCRC2: Cytochrome b-c1 complex subunit 2, UQCRFS1: Cytochrome b-c1 complex subunit Rieske, UROD:
683 Uroporphynogen decarboxylase, UROgenIII: Uroporphyrinogen III, UROS: Uroporphyrinogen Synthase
684

685 **Author Contributions:** methodology, A.G.; data curation, N.T., J.M.H; writing—original draft preparation, N.T,
686 J.M.H, N.L.; writing—review and editing, N.L, S.B and B.M.; supervision, project administration, funding
687 acquisition, N.L. All authors have read and agreed to the published version of the manuscript.”

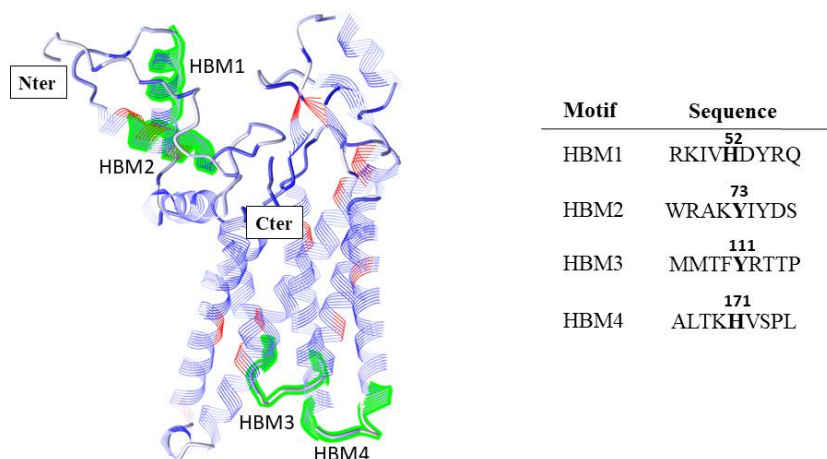
688 **Funding:** This research was funded by UVSQ, EPHE and private funding collected by the UVSQ Foundation.
689 NL received a grant from the UVSQ (AAPSI2019 for the MITOSIDERO project). This work was partly funded
690 by ‘NeurATRIS ANR-11-INBS-0011’, of the French Investissements d’Avenir Program run by the Agence
691 Nationale pour la Recherche.

692 **Acknowledgments:** We acknowledge all the members of the LGBC lab for their support and their contribution
693 to the good atmosphere at work. We are particularly grateful to Juliette Bertheault de Noiron who helped with
694 Fiji macros, Sebastien Szuplewski for its interesting scientific speeches, Christine Wintz for technical assistance
695 and Marie-Pierre Golinelli for giving us DFO. And finally, many thanks to the people who support our research
696 by donating at the UVSQ Foundation.

697 **Conflicts of Interest:** The authors declare no conflict of interest.
698

699 **Appendix A**700 **A.1. Prediction of Heme Binding Motifs in SFXN1**

701 The computational tool *SeqD-HBM* ([131.220.139.55/SeqDHBM/](https://doi.org/10.13140/RJ.2019.0205)) was used for the determination
 702 of heme binding motifs in human SFXN1 (Uniprot entry Q96NB2). The default mode released 13
 703 possible heme-coordination sites and the WESA mode, which passes the sequence through a
 704 sequence-based solvent accessibility meta-predictor, gave 4 putative HBMs. These putative HBMs
 705 were further located on SFXN1 predicted structure, highlighting 4 sites that may transiently interact
 706 with heme (**Figure S1**). If our predictions are correct, two sites would be located in the matrix and
 707 the others would be in the intermembrane space.
 708



709
 710
 711 **Figure S1. Predicted HBMs in human SFXN1.** *Left panel:* The putative HBMs on SFXN1 predicted structure
 712 are highlighted (in green). *Right panel:* Sequences of the 9mer motifs in SFXN1 corresponding to predicted HBMs.
 713 The position of the potential heme-coordination site (Cys, His or Tyr) is shown (bold).
 714

715 **A.2. Mitochondrial labile iron staining with the MitoFerro-Green fluorescent probe**

716 Prior to the staining, HT1080 cells were seeded in a 6-well plate and transiently transfected with
 717 a validated scrambled control siRNA (Control siRNA-A sc-37007, Santa Cruz Biotechnology, INC) or
 718 a pool of specific siRNA for SFXN1 (sc-91814, Santa Cruz Biotechnology, INC) using Interferin™
 719 transfection reagent (Polyplus-transfection Inc., New York, NY) following manufacturer instructions.
 720 Briefly, a mix of siRNA and Interferin™ transfection reagent was prepared and incubated for 10 min
 721 at room temperature, and then, added to each well at a final concentration of 10 nM. Cells were
 722 incubated at 37°C under standard culture conditions and amplified. 24h post-transfection, cells were
 723 seeded in μ -Slide 2 Well (Ibidi) and further incubated at 37°C under standard culture conditions for
 724 24 h. The following day, cells were eventually treated with deferoxamine (DFO) with or without
 725 FeCl₃ for 1h30 or erastin for 6 h before adding the MitoFerro-Green probe (Dojindo, TEBU, France).
 726 MitoFerro-Green staining was done according to the manufacturer's recommendations. Live imaging
 727 images were acquired on a Leica TCS SPE confocal microscope with a 63X oil immersion objective
 728 (CYMAGES imaging facility, UVSQ). Image analysis of three independent experiments was done
 729 using ImageJ software with a macro developed in the lab.
 730

731 **References**

- 732 1. Fleming, M.D. A Mutation in a Mitochondrial Transmembrane Protein Is Responsible for the
733 Pleiotropic Hematological and Skeletal Phenotype of Flexed-Tail (*f/f*) Mice. *Genes & Development* **2001**, *15*,
734 652–657, doi:10.1101/gad.873001.
- 735 2. Lenox, L.E.; Perry, J.M.; Paulson, R.F. BMP4 and Madh5 Regulate the Erythroid Response to Acute
736 Anemia. *Blood* **2005**, *105*, 2741–2748, doi:10.1182/blood-2004-02-0703.
- 737 3. Hegde, S.; Lenox, L.E.; Lariviere, A.; Porayette, P.; Perry, J.M.; Yon, M.; Paulson, R.F. An Intronic
738 Sequence Mutated in Flexed-Tail Mice Regulates Splicing of Smad5. *Mamm Genome* **2007**, *18*, 852–860,
739 doi:10.1007/s00335-007-9074-9.
- 740 4. SLC56 Sideroflexins. IUPHAR/BPS Guide to PHARMACOLOGY 2020.
- 741 5. Li, X.; Han, D.; Kin Ting Kam, R.; Guo, X.; Chen, M.; Yang, Y.; Zhao, H.; Chen, Y. Developmental
742 Expression of Sideroflexin Family Genes in *Xenopus* Embryos. *Dev. Dyn.* **2010**, *239*, 2742–2747,
743 doi:10.1002/dvdy.22401.
- 744 6. Lockhart, P.J.; Holtom, B.; Lincoln, S.; Hussey, J.; Zimprich, A.; Gasser, T.; Wszolek, Z.K.; Hardy, J.;
745 Farrer, M.J. The Human Sideroflexin 5 (SFXN5) Gene: Sequence, Expression Analysis and Exclusion as a
746 Candidate for PARK3. *Gene* **2002**, *285*, 229–237.
- 747 7. Miotto, G.; Tessaro, S.; Rotta, G.A.; Bonatto, D. In Silico Analyses of Fsf1 Sequences, a New Group of
748 Fungal Proteins Orthologous to the Metazoan Sideroblastic Anemia-Related Sideroflexin Family. *Fungal*
749 *Genet. Biol.* **2007**, *44*, 740–753, doi:10.1016/j.fgb.2006.12.004.
- 750 8. Kory, N.; Wyant, G.A.; Prakash, G.; uit de Bos, J.; Bottanelli, F.; Pacold, M.E.; Chan, S.H.; Lewis, C.A.;
751 Wang, T.; Keys, H.R.; et al. SFXN1 Is a Mitochondrial Serine Transporter Required for One-Carbon
752 Metabolism. *Science* **2018**, *362*, eaat9528, doi:10.1126/science.aat9528.
- 753 9. Mon, E.E.; Wei, F.-Y.; Ahmad, R.N.R.; Yamamoto, T.; Moroishi, T.; Tomizawa, K. Regulation of
754 Mitochondrial Iron Homeostasis by Sideroflexin 2. *The Journal of Physiological Sciences* **2019**, *69*, 359–373,
755 doi:10.1007/s12576-018-0652-2.
- 756 10. Gyimesi, G.; Hediger, M.A. Sequence Features of Mitochondrial Transporter Protein Families.
757 *Biomolecules* **2020**, *10*, 1611, doi:10.3390/biom10121611.
- 758 11. Yang, J.; Anishchenko, I.; Park, H.; Peng, Z.; Ovchinnikov, S.; Baker, D. Improved Protein Structure
759 Prediction Using Predicted Interresidue Orientations. *Proc Natl Acad Sci USA* **2020**, *117*, 1496–1503,
760 doi:10.1073/pnas.1914677117.
- 761 12. Corpet, F. Multiple Sequence Alignment with Hierarchical Clustering. *Nucleic Acids Research* **1988**, *16*,
762 10881–10890, doi:10.1093/nar/16.22.10881.
- 763 13. Yoo, C.-M.; Rhee, H.-W. APEX, a Master Key to Resolve Membrane Topology in Live Cells.
764 *Biochemistry* **2019**, acs.biochem.9b00785, doi:10.1021/acs.biochem.9b00785.
- 765 14. Lee, S.-Y.; Kang, M.-G.; Park, J.-S.; Lee, G.; Ting, A.Y.; Rhee, H.-W. APEX Fingerprinting Reveals the
766 Subcellular Localization of Proteins of Interest. *Cell Reports* **2016**, *15*, 1837–1847,
767 doi:10.1016/j.celrep.2016.04.064.
- 768 15. Acoba, M.G.; Selen Alpergin, E.S.; Renuse, S.; Fernández-del-Río, L.; Lu, Y.-W.; Clarke, C.F.; Pandey,
769 A.; Wolfgang, M.J.; Claypool, S.M. *The Mitochondrial Carrier SFXN1 Is Critical for Complex III Integrity and*
770 *Cellular Metabolism*; Biochemistry, 2020;
- 771 16. Jackson, T.D.; Hock, D.; Palmer, C.S.; Kang, Y.; Fujihara, K.M.; Clemons, N.J.; Thorburn, D.R.; Stroud,
772 D.A.; Stojanovski, D. *The TIM22 Complex Regulates Mitochondrial One-Carbon Metabolism by Mediating the*
773 *Import of Sideroflexins*; Cell Biology, 2020;
- 774 17. Azzi, A.; Glerum, M.; Koller, R.; Mertens, W.; Spycher, S. The Mitochondrial Tricarboxylate Carrier. *J*
775 *Bioenerg Biomembr* **1993**, *25*, 515–524, doi:10.1007/BF01108408.
- 776 18. Miyake, S.; Yamashita, T.; Taniguchi, M.; Tamatani, M.; Sato, K.; Tohyama, M. Identification and
777 Characterization of a Novel Mitochondrial Tricarboxylate Carrier. *Biochemical and Biophysical Research*
778 *Communications* **2002**, *295*, 463–468, doi:10.1016/S0006-291X(02)00694-0.
- 779 19. Kovaleva, G.Yu.; Bazykin, G.A.; Brudno, M.; Gelfand, M.S. COMPARATIVE GENOMICS OF
780 TRANSCRIPTIONAL REGULATION IN YEASTS AND ITS APPLICATION TO IDENTIFICATION OF A
781 CANDIDATE ALPHA-ISOPROPYLMALATE TRANSPORTER. *Journal of Bioinformatics and Computational*
782 *Biology* **2006**, *04*, 981–998, doi:10.1142/S0219720006002284.

- 783 20. Wood, V.; Harris, M.A.; McDowall, M.D.; Rutherford, K.; Vaughan, B.W.; Staines, D.M.; Aslett, M.;
784 Lock, A.; Bahler, J.; Kersey, P.J.; et al. PomBase: A Comprehensive Online Resource for Fission Yeast. *Nucleic*
785 *Acids Research* **2012**, *40*, D695–D699, doi:10.1093/nar/gkr853.
- 786 21. Lock, A.; Rutherford, K.; Harris, M.A.; Hayles, J.; Oliver, S.G.; Bähler, J.; Wood, V. PomBase 2018:
787 User-Driven Reimplementation of the Fission Yeast Database Provides Rapid and Intuitive Access to
788 Diverse, Interconnected Information. *Nucleic Acids Research* **2019**, *47*, D821–D827, doi:10.1093/nar/gky961.
- 789 22. Ye, X.; Xu, J.; Cheng, C.; Yin, G.; Zeng, L.; Ji, C.; Gu, S.; Xie, Y.; Mao, Y. Isolation and Characterization
790 of a Novel Human Putative Anemia-Related Gene Homologous to Mouse Sideroflexin. *Biochem. Genet.*
791 **2003**, *41*, 119–125.
- 792 23. Whittaker, M.M.; Penmatsa, A.; Whittaker, J.W. The Mtm1p Carrier and Pyridoxal 5'-Phosphate
793 Cofactor Trafficking in Yeast Mitochondria. *Archives of Biochemistry and Biophysics* **2015**, *568*, 64–70,
794 doi:10.1016/j.abb.2015.01.021.
- 795 24. Whittaker, J.W. Intracellular Trafficking of the Pyridoxal Cofactor. Implications for Health and
796 Metabolic Disease. *Archives of Biochemistry and Biophysics* **2016**, *592*, 20–26, doi:10.1016/j.abb.2015.11.031.
- 797 25. Curcio, R.; Lunetti, P.; Zara, V.; Ferramosca, A.; Marra, F.; Fiermonte, G.; Cappello, A.R.; De
798 Leonardis, F.; Capobianco, L.; Dolce, V. Drosophila Melanogaster Mitochondrial Carriers: Similarities and
799 Differences with the Human Carriers. *IJMS* **2020**, *21*, 6052, doi:10.3390/ijms21176052.
- 800 26. Wang, J.; Youkharibache, P.; Zhang, D.; Lanczycki, C.J.; Geer, R.C.; Madej, T.; Phan, L.; Ward, M.; Lu,
801 S.; Marchler, G.H.; et al. ICn3D, a Web-Based 3D Viewer for Sharing 1D/2D/3D Representations of
802 Biomolecular Structures. *Bioinformatics* **2020**, *36*, 131–135, doi:10.1093/bioinformatics/btz502.
- 803 27. Rivell, A.; Petralia, R.S.; Wang, Y.-X.; Mattson, M.P.; Yao, P.J. Sideroflexin 3 Is a Mitochondrial Protein
804 Enriched in Neurons. *Neuromol Med* **2019**, *21*, 314–321, doi:10.1007/s12017-019-08553-7.
- 805 28. Hildick-Smith, G.J.; Cooney, J.D.; Garone, C.; Kremer, L.S.; Haack, T.B.; Thon, J.N.; Miyata, N.; Lieber,
806 D.S.; Calvo, S.E.; Akman, H.O.; et al. Macrocytic Anemia and Mitochondriopathy Resulting from a Defect
807 in Sideroflexin 4. *Am. J. Hum. Genet.* **2013**, *93*, 906–914, doi:10.1016/j.ajhg.2013.09.011.
- 808 29. Fecher, C.; Trovò, L.; Müller, S.A.; Snaidero, N.; Wettmarshausen, J.; Heink, S.; Ortiz, O.; Wagner, I.;
809 Kühn, R.; Hartmann, J.; et al. Cell-Type-Specific Profiling of Brain Mitochondria Reveals Functional and
810 Molecular Diversity. *Nat Neurosci* **2019**, *22*, 1731–1742, doi:10.1038/s41593-019-0479-z.
- 811 30. Sofou, K.; Hedberg-Oldfors, C.; Kollberg, G.; Thomsen, C.; Wiksell, Å.; Oldfors, A.; Tulinius, M.
812 Prenatal onset of mitochondrial disease is associated with sideroflexin 4 deficiency. *Mitochondrion* **2019**, *47*,
813 76–81, doi:10.1016/j.mito.2019.04.012.
- 814 31. Paul, B.T.; Tesfay, L.; Winkler, C.R.; Torti, F.M.; Torti, S.V. Sideroflexin 4 Affects Fe-S Cluster
815 Biogenesis, Iron Metabolism, Mitochondrial Respiration and Heme Biosynthetic Enzymes. *Sci Rep* **2019**, *9*,
816 19634, doi:10.1038/s41598-019-55907-z.
- 817 32. Gylfe, A.E.; Katainen, R.; Kondelin, J.; Tanskanen, T.; Cajuso, T.; Hänninen, U.; Taipale, J.; Taipale, M.;
818 Renkonen-Sinisalo, L.; Järvinen, H.; et al. Eleven Candidate Susceptibility Genes for Common Familial
819 Colorectal Cancer. *PLoS Genet* **2013**, *9*, doi:10.1371/journal.pgen.1003876.
- 820 33. Weston, C.; Klobusicky, J.; Weston, J.; Connor, J.; Toms, S.A.; Marko, N.F. Aberrations in the Iron
821 Regulatory Gene Signature Are Associated with Decreased Survival in Diffuse Infiltrating Gliomas. *PLoS*
822 *ONE* **2016**, *11*, e0166593, doi:10.1371/journal.pone.0166593.
- 823 34. Miller, L.D.; Coffman, L.G.; Chou, J.W.; Black, M.A.; Bergh, J.; D'Agostino, R.; Torti, S.V.; Torti, F.M.
824 An Iron Regulatory Gene Signature Predicts Outcome in Breast Cancer. *Cancer Res* **2011**, *71*, 6728–6737,
825 doi:10.1158/0008-5472.CAN-11-1870.
- 826 35. Wu, M.; Gu, J.; Zong, S.; Guo, R.; Liu, T.; Yang, M. Research Journey of Respirasome. *Protein Cell* **2020**,
827 *11*, 318–338, doi:10.1007/s13238-019-00681-x.
- 828 36. Guo, R.; Gu, J.; Zong, S.; Wu, M.; Yang, M. Structure and Mechanism of Mitochondrial Electron
829 Transport Chain. *Biomedical Journal* **2018**, *41*, 9–20, doi:10.1016/j.bj.2017.12.001.
- 830 37. Stiban, J.; So, M.; Kaguni, L.S. Iron-Sulfur Clusters in Mitochondrial Metabolism: Multifaceted Roles
831 of a Simple Cofactor. *Biochemistry Moscow* **2016**, *81*, 1066–1080, doi:10.1134/S0006297916100059.
- 832 38. Barros, M.H.; McStay, G.P. Modular Biogenesis of Mitochondrial Respiratory Complexes.
833 *Mitochondrion* **2020**, *50*, 94–114, doi:10.1016/j.mito.2019.10.008.
- 834 39. Letts, J.A.; Sazanov, L.A. Clarifying the Supercomplex: The Higher-Order Organization of the
835 Mitochondrial Electron Transport Chain. *Nat Struct Mol Biol* **2017**, *24*, 800–808, doi:10.1038/nsmb.3460.

- 836 40. Ndi, M.; Marin-Buera, L.; Salvatori, R.; Singh, A.P.; Ott, M. Biogenesis of the Bc1 Complex of the
837 Mitochondrial Respiratory Chain. *Journal of Molecular Biology* **2018**, *430*, 3892–3905,
838 doi:10.1016/j.jmb.2018.04.036.
- 839 41. Sánchez, E.; Lobo, T.; Fox, J.L.; Zeviani, M.; Winge, D.R.; Fernández-Vizarra, E. LYRM7/MZM1L Is a
840 UQCRCFS1 Chaperone Involved in the Last Steps of Mitochondrial Complex III Assembly in Human Cells.
841 *Biochimica et Biophysica Acta (BBA) - Bioenergetics* **2013**, *1827*, 285–293, doi:10.1016/j.bbabo.2012.11.003.
- 842 42. Tang, W.K.; Borgnia, M.J.; Hsu, A.L.; Esser, L.; Fox, T.; de Val, N.; Xia, D. Structures of AAA Protein
843 Translocase Bcs1 Suggest Translocation Mechanism of a Folded Protein. *Nat Struct Mol Biol* **2020**, *27*, 202–
844 209, doi:10.1038/s41594-020-0373-0.
- 845 43. Wang, Y.; Hekimi, S. Understanding Ubiquinone. *Trends in Cell Biology* **2016**, *26*, 367–378,
846 doi:10.1016/j.tcb.2015.12.007.
- 847 44. Visapää, I.; Fellman, V.; Vesa, J.; Dasvarma, A.; Hutton, J.L.; Kumar, V.; Payne, G.S.; Makarow, M.;
848 Van Coster, R.; Taylor, R.W.; et al. GRACILE Syndrome, a Lethal Metabolic Disorder with Iron Overload,
849 Is Caused by a Point Mutation in BCS1L. *The American Journal of Human Genetics* **2002**, *71*, 863–876,
850 doi:10.1086/342773.
- 851 45. Amorim, I.S.; Graham, L.C.; Carter, R.N.; Morton, N.M.; Hammachi, F.; Kunath, T.; Pennetta, G.;
852 Carpanini, S.M.; Manson, J.C.; Lamont, D.J.; et al. Sideroflexin 3 Is an α -Synuclein-Dependent
853 Mitochondrial Protein That Regulates Synaptic Morphology. *J. Cell. Sci.* **2017**, *130*, 325–331,
854 doi:10.1242/jcs.194241.
- 855 46. Ducker, G.S.; Rabinowitz, J.D. One-Carbon Metabolism in Health and Disease. *Cell Metabolism* **2017**,
856 *25*, 27–42, doi:10.1016/j.cmet.2016.08.009.
- 857 47. Minton, D.R.; Nam, M.; McLaughlin, D.J.; Shin, J.; Bayraktar, E.C.; Alvarez, S.W.; Sviderskiy, V.O.;
858 Papagiannakopoulos, T.; Sabatini, D.M.; Birsoy, K.; et al. Serine Catabolism by SHMT2 Is Required for
859 Proper Mitochondrial Translation Initiation and Maintenance of Formylmethionyl-TRNAs. *Molecular Cell*
860 **2018**, *69*, 610–621.e5, doi:10.1016/j.molcel.2018.01.024.
- 861 48. Antoniewicz, M.R. A Guide to ¹³C Metabolic Flux Analysis for the Cancer Biologist. *Exp Mol Med*
862 **2018**, *50*, 19, doi:10.1038/s12276-018-0060-y.
- 863 49. Plaitakis, A.; Kalef-Ezra, E.; Kotzamani, D.; Zaganas, I.; Spanaki, C. The Glutamate Dehydrogenase
864 Pathway and Its Roles in Cell and Tissue Biology in Health and Disease. *Biology* **2017**, *6*, 11,
865 doi:10.3390/biology6010011.
- 866 50. Smith, H.Q.; Li, C.; Stanley, C.A.; Smith, T.J. Glutamate Dehydrogenase, a Complex Enzyme at a
867 Crucial Metabolic Branch Point. *Neurochem Res* **2019**, *44*, 117–132, doi:10.1007/s11064-017-2428-0.
- 868 51. Kurmi, K.; Haigis, M.C. Nitrogen Metabolism in Cancer and Immunity. *Trends in Cell Biology* **2020**, *30*,
869 408–424, doi:10.1016/j.tcb.2020.02.005.
- 870 52. Richardson, D.R.; Lane, D.J.R.; Becker, E.M.; Huang, M.L.-H.; Whitnall, M.; Rahmanto, Y.S.; Sheftel,
871 A.D.; Ponka, P. Mitochondrial Iron Trafficking and the Integration of Iron Metabolism between the
872 Mitochondrion and Cytosol. *Proceedings of the National Academy of Sciences* **2010**, *107*, 10775–10782,
873 doi:10.1073/pnas.0912925107.
- 874 53. Torti, S.V.; Torti, F.M. Iron and Cancer: More Ore to Be Mined. *Nat Rev Cancer* **2013**, *13*, 342–355,
875 doi:10.1038/nrc3495.
- 876 54. Paul, B.T.; Manz, D.H.; Torti, F.M.; Torti, S.V. Mitochondria and Iron: Current Questions. *Expert*
877 *Review of Hematology* **2017**, *10*, 65–79, doi:10.1080/17474086.2016.1268047.
- 878 55. Kafina, M.D.; Paw, B.H. Intracellular Iron and Heme Trafficking and Metabolism in Developing
879 Erythroblasts. *Metallomics* **2017**, *9*, 1193–1203, doi:10.1039/C7MT00103G.
- 880 56. Muckenthaler, M.U.; Galy, B.; Hentze, M.W. Systemic Iron Homeostasis and the Iron-Responsive
881 Element/Iron-Regulatory Protein (IRE/IRP) Regulatory Network. *Annu. Rev. Nutr.* **2008**, *28*, 197–213,
882 doi:10.1146/annurev.nutr.28.061807.155521.
- 883 57. Tong, W.-H.; Rouault, T.A. Metabolic Regulation of Citrate and Iron by Aconitases: Role of Iron-
884 Sulfur Cluster Biogenesis. *Biometals* **2007**, *20*, 549–564, doi:10.1007/s10534-006-9047-6.
- 885 58. Zhou, Z.D.; Tan, E.-K. Iron Regulatory Protein (IRP)-Iron Responsive Element (IRE) Signaling
886 Pathway in Human Neurodegenerative Diseases. *Mol Neurodegener* **2017**, *12*, 75, doi:10.1186/s13024-017-
887 0218-4.
- 888 59. Lill, R.; Mühlenhoff, U. Maturation of Iron-Sulfur Proteins in Eukaryotes: Mechanisms, Connected
889 Processes, and Diseases. *Annu. Rev. Biochem.* **2008**, *77*, 669–700,
890 doi:10.1146/annurev.biochem.76.052705.162653.

- 891 60. Beinert, H.; Kennedy, M.C.; Stout, C.D. Aconitase as Iron-Sulfur Protein, Enzyme, and Iron-
892 Regulatory Protein. *Chem. Rev.* **1996**, *96*, 2335–2374, doi:10.1021/cr950040z.
- 893 61. Netz, D.J.A.; Stith, C.M.; Stümpfig, M.; Köpf, G.; Vogel, D.; Genau, H.M.; Stodola, J.L.; Lill, R.; Burgers,
894 P.M.J.; Pierik, A.J. Eukaryotic DNA Polymerases Require an Iron-Sulfur Cluster for the Formation of Active
895 Complexes. *Nat Chem Biol* **2012**, *8*, 125–132, doi:10.1038/nchembio.721.
- 896 62. Rudolf, J.; Makranton, V.; Ingledew, W.J.; Stark, M.J.R.; White, M.F. The DNA Repair Helicases XPD
897 and FancJ Have Essential Iron-Sulfur Domains. *Molecular Cell* **2006**, *23*, 801–808,
898 doi:10.1016/j.molcel.2006.07.019.
- 899 63. Rouault, T.A. Biogenesis of Iron-Sulfur Clusters in Mammalian Cells: New Insights and Relevance to
900 Human Disease. *Disease Models & Mechanisms* **2012**, *5*, 155–164, doi:10.1242/dmm.009019.
- 901 64. Guengerich, F.P. Cytochrome P450 Research and *The Journal of Biological Chemistry*. *J. Biol. Chem.* **2019**,
902 *294*, 1671–1680, doi:10.1074/jbc.TM118.004144.
- 903 65. Lin, Y.-W. Structure and Function of Heme Proteins Regulated by Diverse Post-Translational
904 Modifications. *Archives of Biochemistry and Biophysics* **2018**, *641*, 1–30, doi:10.1016/j.abb.2018.01.009.
- 905 66. Poulos, T.L. Heme Enzyme Structure and Function. *Chem. Rev.* **2014**, *114*, 3919–3962,
906 doi:10.1021/cr400415k.
- 907 67. Ajioka, R.S.; Phillips, J.D.; Kushner, J.P. Biosynthesis of Heme in Mammals. *Biochimica et Biophysica*
908 *Acta (BBA) - Molecular Cell Research* **2006**, *1763*, 723–736, doi:10.1016/j.bbamcr.2006.05.005.
- 909 68. Stojanovski, B.M.; Hunter, G.A.; Na, I.; Uversky, V.N.; Jiang, R.H.Y.; Ferreira, G.C. 5-Aminolevulinate
910 Synthase Catalysis: The Catcher in Heme Biosynthesis. *Molecular Genetics and Metabolism* **2019**, *128*, 178–
911 189, doi:10.1016/j.ymgme.2019.06.003.
- 912 69. Swenson, S.A.; Moore, C.M.; Marcero, J.R.; Medlock, A.E.; Reddi, A.R.; Khalimonchuk, O. From
913 Synthesis to Utilization: The Ins and Outs of Mitochondrial Heme. *Cells* **2020**, *9*, 579,
914 doi:10.3390/cells9030579.
- 915 70. Hirayama, T.; Kadota, S.; Niwa, M.; Nagasawa, H. A Mitochondria-Targeted Fluorescent Probe for
916 Selective Detection of Mitochondrial Labile Fe(II). *Metallomics* **2018**, *10*, 794–801, doi:10.1039/C8MT00049B.
- 917 71. Nishizawa, H.; Matsumoto, M.; Shindo, T.; Saigusa, D.; Kato, H.; Suzuki, K.; Sato, M.; Ishii, Y.;
918 Shimokawa, H.; Igarashi, K. Ferroptosis Is Controlled by the Coordinated Transcriptional Regulation of
919 Glutathione and Labile Iron Metabolism by the Transcription Factor BACH1. *J. Biol. Chem.* **2020**, *295*, 69–
920 82, doi:10.1074/jbc.RA119.009548.
- 921 72. Kwon, M.-Y.; Park, E.; Lee, S.-J.; Chung, S.W. Heme Oxygenase-1 Accelerates Erastin-Induced
922 Ferroptotic Cell Death. *Oncotarget* **2015**, *6*, 24393–24403, doi:10.18632/oncotarget.5162.
- 923 73. Ichikawa, Y.; Bayeva, M.; Ghanefar, M.; Potini, V.; Sun, L.; Mutharasan, R.K.; Wu, R.; Khechaduri, A.;
924 Jairaj Naik, T.; Ardehali, H. Disruption of ATP-Binding Cassette B8 in Mice Leads to Cardiomyopathy
925 through a Decrease in Mitochondrial Iron Export. *Proceedings of the National Academy of Sciences* **2012**, *109*,
926 4152–4157, doi:10.1073/pnas.1119338109.
- 927 74. Lunetti, P.; Damiano, F.; De Benedetto, G.; Siculella, L.; Pennetta, A.; Muto, L.; Paradies, E.; Marobbio,
928 C.M.T.; Dolce, V.; Capobianco, L. Characterization of Human and Yeast Mitochondrial Glycine Carriers
929 with Implications for Heme Biosynthesis and Anemia. *Journal of Biological Chemistry* **2016**, *291*, 19746–19759,
930 doi:10.1074/jbc.M116.736876.
- 931 75. Ulrich, D.L.; Lynch, J.; Wang, Y.; Fukuda, Y.; Nachagari, D.; Du, G.; Sun, D.; Fan, Y.; Tsurkan, L.;
932 Potter, P.M.; et al. ATP-Dependent Mitochondrial Porphyrin Importer ABCB6 Protects against
933 Phenylhydrazine Toxicity. *J. Biol. Chem.* **2012**, *287*, 12679–12690, doi:10.1074/jbc.M111.336180.
- 934 76. Yamamoto, M.; Arimura, H.; Fukushige, T.; Minami, K.; Nishizawa, Y.; Tanimoto, A.; Kanekura, T.;
935 Nakagawa, M.; Akiyama, S. -i.; Furukawa, T. Abcb10 Role in Heme Biosynthesis In Vivo: Abcb10 Knockout
936 in Mice Causes Anemia with Protoporphyrin IX and Iron Accumulation. *Molecular and Cellular Biology* **2014**,
937 *34*, 1077–1084, doi:10.1128/MCB.00865-13.
- 938 77. Wißbrock, A.; Paul George, A.A.; Brewitz, H.H.; Köhl, T.; Imhof, D. The Molecular Basis of Transient
939 Heme-Protein Interactions: Analysis, Concept and Implementation. *Bioscience Reports* **2019**, *39*,
940 BSR20181940, doi:10.1042/BSR20181940.
- 941 78. Paul George, A.A.; Lacerda, M.; Syllwasschy, B.F.; Hopp, M.-T.; Wißbrock, A.; Imhof, D. HeMoQuest:
942 A Webserver for Qualitative Prediction of Transient Heme Binding to Protein Motifs. *BMC Bioinformatics*
943 **2020**, *21*, 124, doi:10.1186/s12859-020-3420-2.

- 944 79. Kubota, Y.; Nomura, K.; Katoh, Y.; Yamashita, R.; Kaneko, K.; Furuyama, K. Novel Mechanisms for
945 Heme-Dependent Degradation of ALAS1 Protein as a Component of Negative Feedback Regulation of
946 Heme Biosynthesis. *J. Biol. Chem.* **2016**, *291*, 20516–20529, doi:10.1074/jbc.M116.719161.
- 947 80. Tretter, L.; Adam-Vizi, V. Alpha-Ketoglutarate Dehydrogenase: A Target and Generator of Oxidative
948 Stress. *Phil. Trans. R. Soc. B* **2005**, *360*, 2335–2345, doi:10.1098/rstb.2005.1764.
- 949 81. Bulteau, A.-L. Frataxin Acts as an Iron Chaperone Protein to Modulate Mitochondrial Aconitase
950 Activity. *Science* **2004**, *305*, 242–245, doi:10.1126/science.1098991.
- 951 82. Mochel, F.; Knight, M.A.; Tong, W.-H.; Hernandez, D.; Ayyad, K.; Taivassalo, T.; Andersen, P.M.;
952 Singleton, A.; Rouault, T.A.; Fischbeck, K.H.; et al. Splice Mutation in the Iron-Sulfur Cluster Scaffold
953 Protein ISCU Causes Myopathy with Exercise Intolerance. *The American Journal of Human Genetics* **2008**, *82*,
954 652–660, doi:10.1016/j.ajhg.2007.12.012.
- 955 83. Taketani, S.; Kakimoto, K.; Ueta, H.; Masaki, R.; Furukawa, T. Involvement of ABC7 in the
956 Biosynthesis of Heme in Erythroid Cells: Interaction of ABC7 with Ferrochelatase. *Blood* **2003**, *101*, 3274–
957 3280, doi:10.1182/blood-2002-04-1212.
- 958 84. Gervason, S.; Larkem, D.; Mansour, A.B.; Botzanowski, T.; Müller, C.S.; Pecqueur, L.; Le Pavec, G.;
959 Delaunay-Moisan, A.; Brun, O.; Agramunt, J.; et al. Physiologically Relevant Reconstitution of Iron-Sulfur
960 Cluster Biosynthesis Uncovers Persulfide-Processing Functions of Ferredoxin-2 and Frataxin. *Nat Commun*
961 **2019**, *10*, 3566, doi:10.1038/s41467-019-11470-9.
- 962 85. van den Ecker, D.; Hoffmann, M.; Müting, G.; Maglioni, S.; Herebian, D.; Mayatepek, E.; Ventura, N.;
963 Distelmaier, F. Caenorhabditis Elegans ATAD-3 Modulates Mitochondrial Iron and Heme Homeostasis.
964 *Biochemical and Biophysical Research Communications* **2015**, *467*, 389–394, doi:10.1016/j.bbrc.2015.09.143.
- 965 86. Harel, T.; Yoon, W.H.; Garone, C.; Gu, S.; Coban-Akdemir, Z.; Eldomery, M.K.; Posey, J.E.; Jhangiani,
966 S.N.; Rosenfeld, J.A.; Cho, M.T.; et al. Recurrent De Novo and Biallelic Variation of ATAD3A , Encoding a
967 Mitochondrial Membrane Protein, Results in Distinct Neurological Syndromes. *The American Journal of*
968 *Human Genetics* **2016**, *99*, 831–845, doi:10.1016/j.ajhg.2016.08.007.
- 969 87. Chen, X.; Yu, C.; Kang, R.; Tang, D. Iron Metabolism in Ferroptosis. *Front. Cell Dev. Biol.* **2020**, *8*,
970 590226, doi:10.3389/fcell.2020.590226.
- 971 88. Wang, H.; Liu, C.; Zhao, Y.; Gao, G. Mitochondria Regulation in Ferroptosis. *European Journal of Cell*
972 *Biology* **2020**, *99*, 151058, doi:10.1016/j.ejcb.2019.151058.
- 973 89. Battaglia, A.M.; Chirillo, R.; Aversa, I.; Sacco, A.; Costanzo, F.; Biamonte, F. Ferroptosis and Cancer:
974 Mitochondria Meet the “Iron Maiden” Cell Death. *Cells* **2020**, *9*, 1505, doi:10.3390/cells9061505.
- 975 90. Dixon, S.J.; Lemberg, K.M.; Lamprecht, M.R.; Skouta, R.; Zaitsev, E.M.; Gleason, C.E.; Patel, D.N.;
976 Bauer, A.J.; Cantley, A.M.; Yang, W.S.; et al. Ferroptosis: An Iron-Dependent Form of Nonapoptotic Cell
977 Death. *Cell* **2012**, *149*, 1060–1072, doi:10.1016/j.cell.2012.03.042.
- 978 91. Li, N.; Wang, W.; Zhou, H.; Wu, Q.; Duan, M.; Liu, C.; Wu, H.; Deng, W.; Shen, D.; Tang, Q.
979 Ferritinophagy-Mediated Ferroptosis Is Involved in Sepsis-Induced Cardiac Injury. *Free Radical Biology and*
980 *Medicine* **2020**, *160*, 303–318, doi:10.1016/j.freeradbiomed.2020.08.009.
- 981 92. Doll, S.; Freitas, F.P.; Shah, R.; Aldrovandi, M.; da Silva, M.C.; Ingold, I.; Goya Grocin, A.; Xavier da
982 Silva, T.N.; Panzilius, E.; Scheel, C.H.; et al. FSP1 Is a Glutathione-Independent Ferroptosis Suppressor.
983 *Nature* **2019**, *575*, 693–698, doi:10.1038/s41586-019-1707-0.
- 984 93. Mancias, J.D.; Wang, X.; Gygi, S.P.; Harper, J.W.; Kimmelman, A.C. Quantitative Proteomics Identifies
985 NCOA4 as the Cargo Receptor Mediating Ferritinophagy. *Nature* **2014**, *509*, 105–109,
986 doi:10.1038/nature13148.
- 987 94. Tang, M.; Huang, Z.; Luo, X.; Liu, M.; Wang, L.; Qi, Z.; Huang, S.; Zhong, J.; Chen, J.-X.; Li, L.; et al.
988 Ferritinophagy Activation and Sideroflexin1-Dependent Mitochondria Iron Overload Is Involved in
989 Apelin-13-Induced Cardiomyocytes Hypertrophy. *Free Radical Biology and Medicine* **2019**, *134*, 445–457,
990 doi:10.1016/j.freeradbiomed.2019.01.052.
- 991 95. Hentze, M.W.; Caughman, S.W.; Casey, J.L.; Kodier, D.M.; Rouault, T.A.; Harford, J.B.; Klausner, R.D.
992 A Model for the Structure and Functions of Iron-Responsive Elements. *Gene* **1988**, *72*, 201–208,
993 doi:10.1016/0378-1119(88)90145-X.
- 994 96. Campillos, M.; Cases, I.; Hentze, M.W.; Sanchez, M. SIREs: Searching for Iron-Responsive Elements.
995 *Nucleic Acids Research* **2010**, *38*, W360–W367, doi:10.1093/nar/gkq371.
- 996 97. Henderson, B.R.; Menotti, E.; Bonnard, C.; Kühn, L.C. Optimal Sequence and Structure of Iron-
997 Responsive Elements. Selection of RNA Stem-Loops with High Affinity for Iron Regulatory Factor. *J Biol*
998 *Chem* **1994**, *269*, 17481–17489.

- 999 98. Henderson, B.R.; Menotti, E.; Kühn, L.C. Iron Regulatory Proteins 1 and 2 Bind Distinct Sets of RNA
1000 Target Sequences. *J Biol Chem* **1996**, *271*, 4900–4908, doi:10.1074/jbc.271.9.4900.
- 1001 99. Butt, J.; Kim, H.Y.; Basilion, J.P.; Cohen, S.; Iwai, K.; Philpott, C.C.; Altschul, S.; Klausner, R.D.;
1002 Rouault, T.A. Differences in the RNA Binding Sites of Iron Regulatory Proteins and Potential Target
1003 Diversity. *Proceedings of the National Academy of Sciences* **1996**, *93*, 4345–4349, doi:10.1073/pnas.93.9.4345.
- 1004 100. Ward, R.J.; Zucca, F.A.; Duyn, J.H.; Crichton, R.R.; Zecca, L. The Role of Iron in Brain Ageing and
1005 Neurodegenerative Disorders. *The Lancet Neurology* **2014**, *13*, 1045–1060, doi:10.1016/S1474-4422(14)70117-
1006 6.
- 1007 101. Lee, J.-H.; Lee, M.-S. Brain Iron Accumulation in Atypical Parkinsonian Syndromes: In Vivo MRI
1008 Evidences for Distinctive Patterns. *Front. Neurol.* **2019**, *10*, 74, doi:10.3389/fneur.2019.00074.
- 1009 102. Ayton, S.; Wang, Y.; Diouf, I.; Schneider, J.A.; Brockman, J.; Morris, M.C.; Bush, A.I. Brain Iron Is
1010 Associated with Accelerated Cognitive Decline in People with Alzheimer Pathology. *Mol Psychiatry* **2020**,
1011 *25*, 2932–2941, doi:10.1038/s41380-019-0375-7.
- 1012 103. Bousejra-ElGarah, F.; Bijani, C.; Coppel, Y.; Faller, P.; Hureau, C. Iron(II) Binding to Amyloid- β , the
1013 Alzheimer's Peptide. *Inorg. Chem.* **2011**, *50*, 9024–9030, doi:10.1021/ic201233b.
- 1014 104. Derry, P.J.; Kent, T.A. Correlating Quantitative Susceptibility Mapping with Cognitive Decline in
1015 Alzheimer's Disease. *Brain* **2017**, *140*, 2069–2072, doi:10.1093/brain/awx167.
- 1016 105. Boopathi, S.; Kolandaivel, P. Fe²⁺ Binding on Amyloid β -Peptide Promotes Aggregation: Fe²⁺
1017 Promotes A β Aggregation. *Proteins* **2016**, *84*, 1257–1274, doi:10.1002/prot.25075.
- 1018 106. Uranga, R.M.; Salvador, G.A. Unraveling the Burden of Iron in Neurodegeneration: Intersections with
1019 Amyloid Beta Peptide Pathology. *Oxidative Medicine and Cellular Longevity* **2018**, *2018*, 1–12,
1020 doi:10.1155/2018/2850341.
- 1021 107. Ott, S.; Dziadulewicz, N.; Crowther, D.C. Iron Is a Specific Cofactor for Distinct Oxidation- and
1022 Aggregation-Dependent A Toxicity Mechanisms in a Drosophila Model. *Disease Models & Mechanisms* **2015**,
1023 *8*, 657–667, doi:10.1242/dmm.019042.
- 1024 108. Minjarez, B.; Calderón-González, K.G.; Rustarazo, M.L.V.; Herrera-Aguirre, M.E.; Labra-Barrios,
1025 M.L.; Rincon-Limas, D.E.; Del Pino, M.M.S.; Mena, R.; Luna-Arias, J.P. Identification of Proteins That Are
1026 Differentially Expressed in Brains with Alzheimer's Disease Using ITRAQ Labeling and Tandem Mass
1027 Spectrometry. *J Proteomics* **2016**, *139*, 103–121, doi:10.1016/j.jprot.2016.03.022.
- 1028 109. Simunovic, F.; Yi, M.; Wang, Y.; Macey, L.; Brown, L.T.; Krichevsky, A.M.; Andersen, S.L.; Stephens,
1029 R.M.; Benes, F.M.; Sonntag, K.C. Gene Expression Profiling of Substantia Nigra Dopamine Neurons:
1030 Further Insights into Parkinson's Disease Pathology. *Brain* **2009**, *132*, 1795–1809, doi:10.1093/brain/awn323.
- 1031 110. Cahill, C.M.; Lahiri, D.K.; Huang, X.; Rogers, J.T. Amyloid Precursor Protein and Alpha Synuclein
1032 Translation, Implications for Iron and Inflammation in Neurodegenerative Diseases. *Biochimica et Biophysica*
1033 *Acta (BBA) - General Subjects* **2009**, *1790*, 615–628, doi:10.1016/j.bbagen.2008.12.001.
- 1034 111. Fang, Y.-Y.; Zeng, P.; Qu, N.; Ning, L.-N.; Chu, J.; Zhang, T.; Zhou, X.-W.; Tian, Q. Evidence of Altered
1035 Depression and Dementia-Related Proteins in the Brains of Young Rats after Ovariectomy. *J. Neurochem.*
1036 **2018**, *146*, 703–721, doi:10.1111/jnc.14537.
- 1037 112. Paul, B.T.; Tesfay, L.; Winkler, C.R.; Torti, F.M.; Torti, S.V. Sideroflexin 4 Affects Fe-S Cluster
1038 Biogenesis, Iron Metabolism, Mitochondrial Respiration and Heme Biosynthetic Enzymes. *Sci Rep* **2019**, *9*,
1039 19634, doi:10.1038/s41598-019-55907-z.
- 1040 113. Balachandran, R.C.; Mukhopadhyay, S.; McBride, D.; Veevers, J.; Harrison, F.E.; Aschner, M.; Haynes,
1041 E.N.; Bowman, A.B. Brain Manganese and the Balance between Essential Roles and Neurotoxicity. *J. Biol.*
1042 *Chem.* **2020**, *295*, 6312–6329, doi:10.1074/jbc.REV119.009453.
- 1043 114. Weiland, A.; Wang, Y.; Wu, W.; Lan, X.; Han, X.; Li, Q.; Wang, J. Ferroptosis and Its Role in Diverse
1044 Brain Diseases. *Mol Neurobiol* **2019**, *56*, 4880–4893, doi:10.1007/s12035-018-1403-3.
- 1045 115. Do Van, B.; Gouel, F.; Jonneaux, A.; Timmerman, K.; Gelé, P.; Pétrault, M.; Bastide, M.; Laloux, C.;
1046 Moreau, C.; Bordet, R.; et al. Ferroptosis, a Newly Characterized Form of Cell Death in Parkinson's Disease
1047 That Is Regulated by PKC. *Neurobiology of Disease* **2016**, *94*, 169–178, doi:10.1016/j.nbd.2016.05.011.
- 1048 116. Zhang, Y.-H.; Wang, D.-W.; Xu, S.-F.; Zhang, S.; Fan, Y.-G.; Yang, Y.-Y.; Guo, S.-Q.; Wang, S.; Guo, T.;
1049 Wang, Z.-Y.; et al. α -Lipoic Acid Improves Abnormal Behavior by Mitigation of Oxidative Stress,
1050 Inflammation, Ferroptosis, and Tauopathy in P301S Tau Transgenic Mice. *Redox Biology* **2018**, *14*, 535–548,
1051 doi:10.1016/j.redox.2017.11.001.

- 1052 117. 117. Hambright, W.S.; Fonseca, R.S.; Chen, L.; Na, R.; Ran, Q. Ablation of Ferroptosis Regulator
1053 Glutathione Peroxidase 4 in Forebrain Neurons Promotes Cognitive Impairment and Neurodegeneration.
1054 *Redox Biology* **2017**, *12*, 8–17, doi:10.1016/j.redox.2017.01.021.
- 1055 118. 118. Country, M.W. Retinal Metabolism: A Comparative Look at Energetics in the Retina. *Brain Research*
1056 **2017**, *1672*, 50–57, doi:10.1016/j.brainres.2017.07.025.
- 1057 119. 119. Picard, E.; Daruich, A.; Youale, J.; Courtois, Y.; Behar-Cohen, F. From Rust to Quantum Biology: The
1058 Role of Iron in Retina Physiopathology. *Cells* **2020**, *9*, 705, doi:10.3390/cells9030705.
- 1059 120. 120. Bigot, K.; Gondouin, P.; Bénard, R.; Montagne, P.; Youale, J.; Piazza, M.; Picard, E.; Bordet, T.; Behar-
1060 Cohen, F. Transferrin Non-Viral Gene Therapy for Treatment of Retinal Degeneration. *Pharmaceutics* **2020**,
1061 *12*, 836, doi:10.3390/pharmaceutics12090836.
- 1062 121. 121. Chen, B.; Aredo, B.; Ding, Y.; Zhong, X.; Zhu, Y.; Zhao, C.X.; Kumar, A.; Xing, C.; Gautron, L.; Lyon,
1063 S.; et al. Forward Genetic Analysis Using OCT Screening Identifies *Sfxn3* Mutations Leading to Progressive
1064 Outer Retinal Degeneration in Mice. *Proc Natl Acad Sci USA* **2020**, *117*, 12931–12942,
1065 doi:10.1073/pnas.1921224117.
- 1066